The Winfrith Concrete Model : Beauty or Beast ?
Insights into the Winfrith Concrete Model

Len Schwer
Schwer Engineering & Consulting Services
Len@Schwer.net

April 2011

Introduction

The so called Winfrith concrete model in LS-DYNA (MAT084 and MAT085) provides:

- A basic plasticity model that includes the third stress invariant for consistently treating both triaxial compression and triaxial extension, e.g. Mohr-Coulomb like behavior,
- Uses radial return which omits material dilation, and thus violates Drucker's Postulate for a stable material,
- Includes strain softening in tension with an attempt at regularization via crack opening width or fracture energy,
- Optional strain rate effects: MAT084 includes rate effects and MAT085 does not,
- Concrete tensile cracking with up to three orthogonal crack planes per element; crack viewing is also possible via an auxiliary post-processing file,
- Optional inclusion of so called 'smeared reinforcement.'

This introductory document describes the basic plasticity model, the strain rate formulations and tensile cracking options. The *MAT_WINFRITH_CONCRETE model is another of the so called LS-DYNA 'simple input' concrete models, that include the *MAT_PSEUDO_TENSOR (MAT016), *MAT_CONCRETE_DAMAGE_REL3 (MAT072R3) and *MAT_CSCM_CONCRETE (MAT159). The Winfrith model requires the user to specify the unconfined compression and tensile strength.

A note on sign convention: in geomechanics compression is usually considered as positive, since most stress states of interest are compressive. However, the Winfrith model uses the standard engineering mechanics convention of compression as negative.

Ottosen Plasticity Model

The plasticity portion of the Winfrith concrete model is based upon the shear failure surface proposed by Ottosen (1977)[1]:

$$F\left(I_1, J_2, \cos 3\theta\right) = a\frac{J_2}{\left(f_c'\right)^2} + \lambda\frac{\sqrt{J_2}}{f_c'} + b\frac{I_1}{f_c'} - 1 \tag{1}$$

The above is referred to as a four parameter model: the constants a and b which control the meridional shape of the shear failure surface, and $\lambda = \lambda\left(\cos 3\theta\right)$ ranging $-1 \le \cos 3\theta \le +1$ for triaxial compression to triaxial extension control the shape of the shear failure surface on the π-plane. In addition to an explicit dependence on the unconfined compressive strength, f_c', as will

[1] The notation in the present document attempts to follow the notation of Ottosen.

be demonstrated, the constants a and b also depend on the ratio of the unconfined *tensile* strength, f_t', to the unconfined compressive strength.

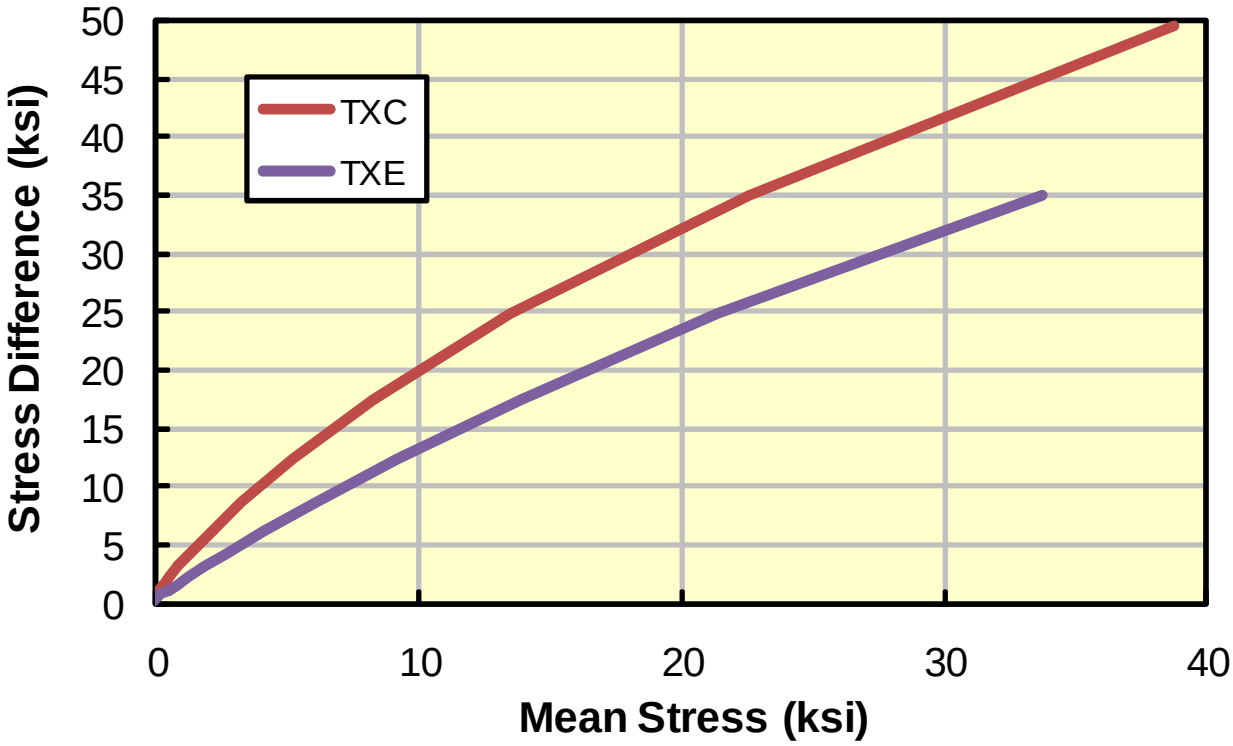

Figure 1 Illustration of Ottosen shear failure surfaces for a 6 ksi unconfined compression strength concrete.

One oddity of the Ottosen shear failure surface is it is both a function J_2 and $\sqrt{J_2}$ unlike almost all other geomaterial shear failure surfaces which are only functions of $\sqrt{J_2}$ .Here J_2 is the second invariant of the deviatoric stress. This makes plotting the traditional view of the shear failure surface in $\left(I_1, \sqrt{J_2}\right)$ space, or alternatively (mean stress, stress difference), a bit different. However, noting Equation (1) is quadratic in the ratio $\sqrt{J_2}/f_c'$ allows for the alternative form of

$$\frac{\sqrt{J_2}}{f_c'} = \frac{-B+\sqrt{B^2-4AC}}{2A}$$
$$A = a$$
$$B = \lambda \qquad (2)$$
$$C = b\frac{I_1}{f_c'} - 1$$

Thus once the parameters a, b, and λ are determined the independent parameter I_1 can be varied to generate the triaxial compression and extension surfaces. Here I_1 is the first invariant of the stress tensor. Figure 1 shows the triaxial compression $(\sigma_1 > \sigma_2 = \sigma_3)$ and triaxial extension $(\sigma_2 = \sigma_3 > \sigma_1)$ surfaces for a f'_c=6 ksi (41 MPa) concrete.

Stress Invariants

To be consistent with the source coding of the Winfrith model, first the invariants of the stress tensor are calculated and then using identities the required invariants of the deviatoric stress tensor are computed.

The stress tensor, σ_{ij}, is assumed to be symmetric with six components:

$$\boldsymbol{\sigma} = \sigma_{ij} = \begin{bmatrix} \sigma_{11} & \sigma_{12} & \sigma_{31} \\ \sigma_{12} & \sigma_{22} & \sigma_{23} \\ \sigma_{31} & \sigma_{23} & \sigma_{33} \end{bmatrix} \tag{3}$$

All third order tensors have three scalar invariants (Eigenvalues), for the stress tensor these are[2]

$$\begin{aligned} I_1 &= \sigma_{kk} = \sigma_{11} + \sigma_{22} + \sigma_{33} \\ I_2 &= 0.5\left(\sigma_{ii}\sigma_{jj} - \sigma_{ij}\sigma_{ji}\right) \\ &= \sigma_{11}\sigma_{22} + \sigma_{22}\sigma_{33} + \sigma_{33}\sigma_{11} - \sigma_{12}^2 - \sigma_{23}^2 - \sigma_{31}^2 \\ I_3 &= DET\left(\sigma_{ij}\right) \\ &= \sigma_{11}\sigma_{22}\sigma_{33} + 2\sigma_{12}\sigma_{23}\sigma_{31} - \sigma_{12}^2\sigma_{33} - \sigma_{23}^2\sigma_{11} - \sigma_{13}^2\sigma_{22} \end{aligned} \tag{4}$$

In constitutive modeling it is often convenient to separate the mean stress (pressure) from the shear response. This is accomplished by introducing the deviatoric stress tensor S_{ij}

$$S_{ij} = \sigma_{ij} - \frac{\sigma_{kk}}{3} \tag{5}$$

Where $\sigma_{kk} = I_1 = 3P$ and P is usually referred to as the mean stress; if all three components of the mean stress are equal then it is referred to as the pressure.

The invariants of the deviatoric stress tensor are related to the stress invariants via the following identities:

[2] See for example http://en.wikipedia.org/wiki/Stress_(mechanics)

$$J_1 = S_{kk} = S_{11} + S_{22} + S_{33} = 0$$
$$J_2 = 0.5 S_{ij} S_{ij} = \frac{1}{3} I_1^2 - I_2 \tag{6}$$
$$J_3 = DET\left(S_{ij}\right) = \frac{2}{27} I_1^3 - \frac{1}{3} I_1 I_2 + I_3$$

Often in the continuum mechanics literature the notation J_2' and J_3' are used with the superscript prime reinforcing the deviatoric stress aspect of the invariants. The third deviatoric stress invariant is rarely used directly, rather a geometric interpretation as an angle in the π-plane with limits $0 \le \theta < \frac{\pi}{3}$ is defined by

$$\cos 3\theta = \frac{3\sqrt{3}}{2} \frac{J_3}{J_2^{1.5}} \tag{7}$$

The angle θ is often referred to as the Lode Angle.

Meridional Shape Parameters

To complete the definition of the shear failure surface given by Equation (1), this section next explains the definition of the meridional shape parameters a and b. As a bit of background these shape parameters can be thought of as best fitting the shear failure surface of laboratory data. The Ottosen model emphasizes simultaneous best fits to four types of laboratory data:

1. Unconfined compression strength, f_c' $\left(\theta = 60^\circ \text{ and } \cos 3\theta = -1\right)$.
2. Uniaxial tensile strength, f_t' $\left(\theta = 0^\circ \text{ and } \cos 3\theta = +1\right)$.
3. Biaxial compressive strength $\left(\sigma_1 = 0, \sigma_2 = \sigma_3 = \text{constant}, \theta = 0\right)$. In particular, the constant stresses are set to $-1.16 f_c'$ corresponding to laboratory tests of Kupfer et al. (1969,1973).
4. A triaxial compression state of stress $\left(\theta = 60^\circ\right)$ which gives the best fit to the data of Balmer (1949) and Richart et al. (1928). The specific point selected has nondimensional coordinates $\left(I_1 / \sqrt{3} f_c',\ \sqrt{2J_2} / f_c'\right) = (-5, 4)$.

The first three laboratory data points are fit exactly and the fourth point is used with a least squares algorithm to obtain a best fit.

In the Winfrith implementation of the Ottosen shear failure surface, the user is not allowed to determine the parameters a and b, but rather the parameters are internally generated based upon an undocumented data fit, and as mentioned above, the ratio of the unconfined tensile to compressive strengths.

The Winfrith model introduces the following three nondimensional constants[3]:

$$\begin{aligned}\alpha &= 1.16 \\ \beta &= 0.5907445 \\ \gamma &= -0.6123724\end{aligned} \tag{8}$$

These constants are used to evaluate the meridional shape parameters a and b:

$$\begin{aligned}b &= \frac{1+R\alpha\frac{\gamma}{3}-\alpha^2\frac{\gamma}{3}-\frac{\alpha}{R}}{\alpha^2\frac{\beta}{3}-3\alpha-R\alpha\frac{\beta}{3}} \\ a &= \beta b+\gamma\end{aligned} \tag{9}$$

Where $R = f_t'/\ f_c' < 1$ is the ratio of the unconfined tensile to compressive strengths.

Octahedral Shape Parameters

The remaining two parameters for this four parameter model are used to define the shape of shear failure surface in the octahedral (π-plane), and these are denoted as k_1 and k_2 in Ottosen's notation. Before defining these two parameters, the Winfrith model introduces two additional constants defined in terms of the above constants a and b:

$$\begin{aligned}c &= \frac{\sqrt{3}}{R}\left(1-bR-R^2\frac{a}{3}\right) \\ d &= \frac{3+3b-a}{\sqrt{3}}\end{aligned} \tag{10}$$

Then the π-plane shape factors are defined as

$$\begin{aligned}k_2 &= \cos\left[3\tan^{-1}\left(\frac{1}{\sqrt{3}}-\frac{2d}{c\sqrt{3}}\right)\right] \\ k_1 &= \frac{c}{\cos\left[\frac{1}{3}\cos^{-1}\left(k_2\right)\right]}\end{aligned} \tag{11}$$

Equations (9) and (11) define the four parameters of the Ottosen shear failure surface.

[3] These are labeled 'low pressure,' an alternative set for 'high pressure' is also provided in the source code but not used.

The function $\lambda = \lambda(\cos 3\theta)$ is now defined in terms of the Lode Angle and the constants k_1 and k_2 as

$$\lambda = \begin{array}{l} k_1 \cos\left[\dfrac{\cos^{-1}(k_2 \cos 3\theta)}{3}\right] \text{ for } \cos 3\theta \geq 0 \\ k_1 \cos\left[\dfrac{\pi}{3} - \dfrac{\cos^{-1}(-k_2 \cos 3\theta)}{3}\right] \text{ for } \cos 3\theta \leq 0 \end{array} \tag{12}$$

Plotting the shear failure surface in the octahedral plane, or π-plane or deviatoric plane, requires a bit more manipulation. In the previous section the meridional shapes of the shear failure surface were plotted by selecting fixed values of the angle θ, often referred to as the *similarity angle* $0 \leq \theta \leq \pi/3$, in particular $\theta = 0$ to generate the triaxial extension surface and $\theta = \pi/3$ to generate the triaxial compression surface. Note: additional surfaces could be drawn for all values of the similarity angle θ.

Octahedral planes are defined by constant values of I_1, or equivalently the mean stress. For such a constant I_1 value, the Ottosen shear failure surface, i.e. Equation (1), is only a function of the $\sqrt{J_2}$ and $\cos 3\theta$. These two parameters can conveniently be thought of as a radius and angle, respectively, in a polar type plot on a octahedral plane. The procedure is to select a value of the similarity angle θ and solve the for corresponding value of $\sqrt{J_2}$ from Equation (1) for the prescribed value of I_1, i.e. a particular octahedral plane. Then the Cartesian equivalent of polar coordinates are defined as

$$\begin{aligned} x &= r\cos\alpha \\ y &= r\sin\alpha \\ r &= \sqrt{2J_2} \\ 0 &\leq \alpha \leq 2\pi \end{aligned} \tag{13}$$

The angle α varies continuously to generate the polar plot and is related to the similarity angle via

$$\begin{aligned} \beta &= \frac{\sin^{-1}(\sin 3\alpha)}{3} \\ \theta &= \beta + \frac{\pi}{6} \end{aligned} \tag{14}$$

Here β is typically referred to as the Lode Angle and varies between $-\pi/6 \leq \beta \leq \pi/6$.

Figure 2 shows an illustration of the octahedral plane shape of the Ottosen shear failure surface. The value $I_1 = -6$ ksi (41 MPa) corresponds to a mean stress of -2 ksi $\left(= P = I_1 / 3\right)$ which is the constant mean stress plane that passes through the intersection of the shear failure surface at the unconfined compression stress trajectory, i.e. $SD = -3P = 6$ ksi $= f_c'$. Note: since the radius used in the octahedral plane is $r = \sqrt{2J_2}$ that radius needs to be scaled by $\sqrt{3}/\sqrt{2} = 1.2247$ to determine the corresponding stress difference value for triaxial loading since $SD = \sqrt{3J_2}$. For example, the maximum triaxial compression value at the bottom of Figure 2 is 4898.98 x 1.2247 = 6000 psi = f_c'.

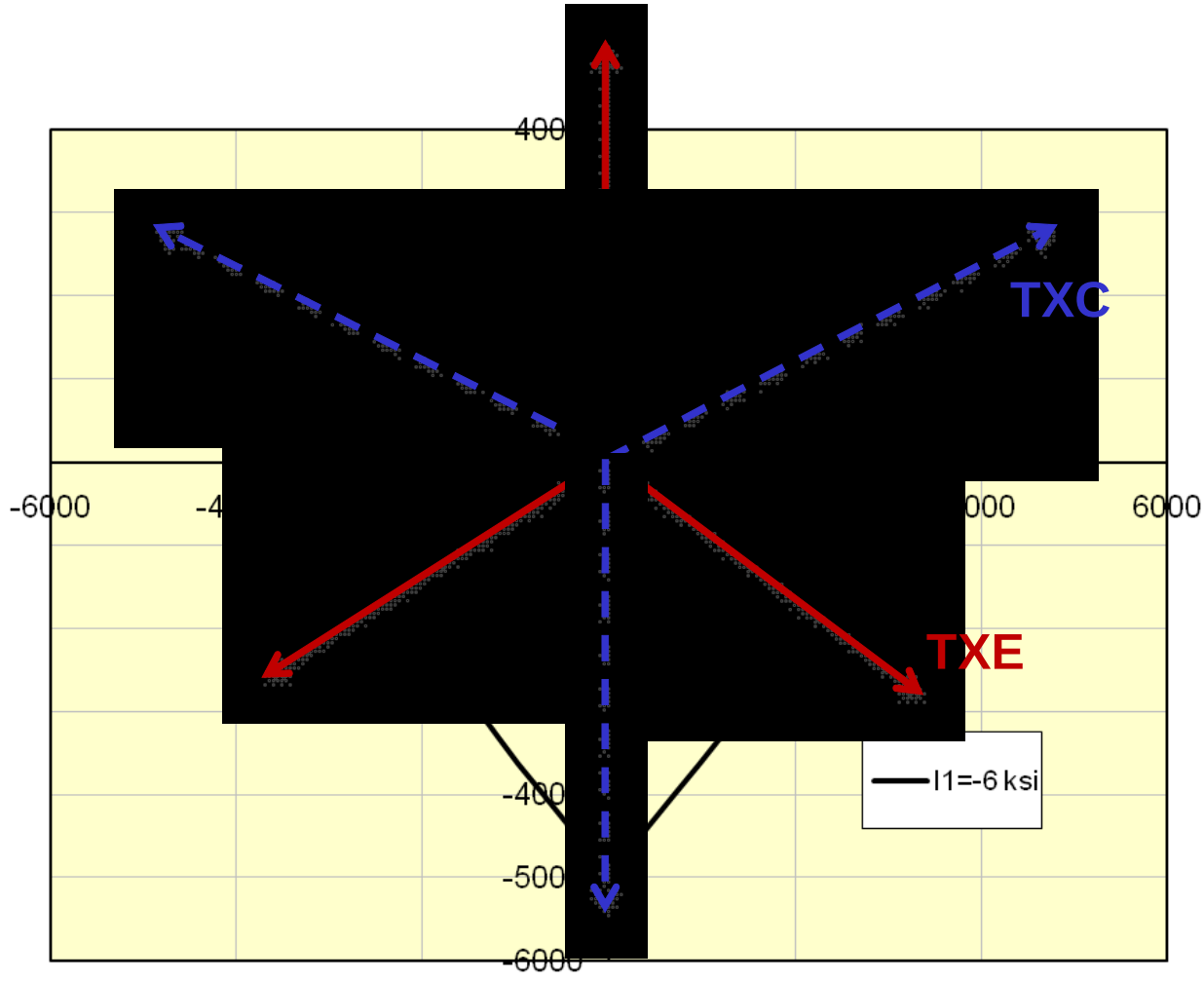

Figure 2 Illustration of the octahedral plane for a 6 ksi (41 MPa) unconfined compression strength concrete.

Pressure versus Volume Strain

The Winfrith concrete model is a so called 'flat cap' model in that in the meridional plane, i.e. $\left(I_1\ ,\ \sqrt{J_2}\right)$, the pressure versus volume strain relation can be represented by a straight line normal to the mean stress axis. While the user may enter up to eight pairs[4] of natural volume strains and corresponding pressures, it is likely users will take advantage of the predefined pressure versus volume strain input option.

The first pair of points in the internally generated pressure versus volume strain is the strain and pressure that occur at the unconfined compression strength, f_c'. The mean stress is at this point is $P_c = f_c'/3$ and the volume strain is approximated as $\varepsilon_c^{vol} = P_c / K$ where the elastic bulk modulus is defined using the user input elastic modulus and Poisson's ratio, viz. $K = E/\left(3(1-2\nu)\right)$. Table 1 provides the ten pressure versus volume strain points generated by the Winfrith model.

Table 1 Winfrith concrete model generated pressure versus volume strain response.

Natural Volume Strain	Pressure (factor multiplies P_c)
$-P_c / K$	1.00
-0.002	1.50
-0.004	3.00
-0.010	4.80
-0.020	6.00
-0.030	7.50
-0.041	9.45
-0.051	11.55
-0.062	14.25
-0.094	25.05

Strain Rate Enhancement

A description of the Winfrith concrete model strain rate enhancement is provided by Broadhouse and Attwood (1993). This paper in turn cites a 1988 CEB Bulletin; the current CEB strain rate enhancement recommendation is provided in CEB (1990). The description presented in this section follows the present coding in the LS-DYNA Winfrith concrete model subroutine.

The strain rate enhancements are based upon the incremental strain rates

$$\dot{\varepsilon}_{ij} = \frac{\Delta\varepsilon_{ij}^n}{\Delta t} \tag{15}$$

[4] Note: the origin point (0,0) may be omitted from the input as this point is treated internally in the Winfrith model.

Where $\Delta\varepsilon_{ij}^{n}$ is the current strain increment obtained from solving the equation of motion and Δt is the current time step n . These incremental strain rates are used to form the incremental effective strain rate $\dot{e}$

$$\begin{aligned}
&\dot{\varepsilon}_{vol} = \dot{\varepsilon}_{kk} = \dot{\varepsilon}_{11} + \dot{\varepsilon}_{22} + \dot{\varepsilon}_{33} \\
&\dot{e}_{ij} = \dot{\varepsilon}_{ij} - \dot{\varepsilon}_{kk}\delta_{ij}/3 \\
&\dot{e} = \sqrt{\frac{2}{3}\dot{e}_{ij}\dot{e}_{ij}} = \sqrt{\frac{2}{3}\left[\dot{e}_{11}^2 + \dot{e}_{22}^2 + \dot{e}_{33}^2 + 0.5\left(\dot{e}_{12}^2 + \dot{e}_{23}^2 + \dot{e}_{31}^2\right)\right]}^{1/2}
\end{aligned} \tag{16}$$

If the incremental effective strain rate is less than 30/second then 'low' strain rate factors are calculated, else if the incremental effective strain rate is greater than 30/second then 'high' strain rate factors are calculated. Note: most strain rate implementations use the plastic portion of the incremental strain and not the total strain increment to minimize noise in the calculation.

For both the low and high strain rates, three strain rate enhancement factors are calculated: tensile E_T , compressive E_C , and Young's modulus E_E :

$$\begin{aligned}
E_T &= \left(\frac{\dot{e}}{\dot{e}_{0T}}\right)^{1.016\delta} \qquad E_C = \left(\frac{\dot{e}}{\dot{e}_{0C}}\right)^{1.026\alpha} \qquad \dot{e} < 30/\mathrm{s} \\
E_T &= \eta\dot{e}^{1/3} \qquad E_C = \gamma\dot{e}^{1/3} \qquad \dot{e} > 30/\mathrm{s}
\end{aligned} \tag{17}$$

Where

$$\begin{aligned}
&\delta = \frac{1}{10 + 0.5 f_{cu}} \\
&\alpha = \frac{1}{5 + 0.75 f_{cu}} \\
&\log_{10}\eta = 6.933\delta - 0.492 \\
&\log_{10}\gamma = 6.156\alpha - 0.492 \\
&\dot{e}_{0T} = 30\times10^{-6}/\mathrm{s} \\
&\dot{e}_{0C} = 3\times10^{-6}/\mathrm{s}
\end{aligned} \tag{18}$$

Here f_{cu} is the concrete cube strength in MPa. Note: concrete cubes rather than cylinders are typically used to determine the unconfined compressive strength in Europe. If f_c' is the cylinder unconfined compressive strength, then $f_{cu} = 1.25 f_c'$ is approximately the corresponding cube strength. In the LS-DYNA implementation the user input uniaxial compressive strength is used as f_{cu} .

The Young's modulus rate enhancement is calculated as an average of tensile and compressive rate enhancements,

$$E_E = 0.5\left[\left(\frac{\dot{e}}{\dot{e}_{0T}}\right)^{0.016} + \left(\frac{\dot{e}}{\dot{e}_{0C}}\right)^{0.026}\right] \tag{19}$$

If any of the above rate enhancement factors are less than one, they are set equal to one, i.e. no rate enhancement.

The following material properties are then rate enhanced

Table 2 Material properties that are strain rate enhanced.

Material Property	Rate Enhancement Factor
Young's modulus	E_E
Shear modulus	E_E
Bulk modulus	E_E
f_c'	E_C
f_t'	E_T

Strain Rate Options

The LS-DYNA implementation of the Winfrith concrete model offers two strain rate options, either to include or omit strain rate effects, selected via the user input parameter RATE. NOTE: rather oddly, RATE=0 turns *on* strain rate effects and RATE=1 turns *off* strain rate effects.

A further consequence of the RATE parameter is the definition of the user input parameter for tensile cracking, FE. When strain rates are turned on, e.g. RATE=0 or *MAT084, the input parameter FE is taken to be the specific fracture energy, i.e. energy per unit area dissipated in opening a crack. When strain rates are turned off, e.g. RATE=1 or *MAT085, the input parameter FE is taken to be the crack width at which the normal, to the crack, tensile stress goes to zero.

Users may be familiar with the fracture energy, associated with Griffith's fracture criterion; the units of the specific fracture energy, denoted here by G_F, are force/length or energy per area. Much less familiar is the other input possibility of the crack width at zero tensile force. It is this Winfrith concrete model input parameter that is the subject of this section.

Note: several respected analysts have reported rather odd results when using the Winfrith model with strain rate effects, i.e. RATE=0, even in quasi-static simulations. The use is cautioned that use of the strain rate option may produce unreliable and inaccurate results.

Crack Width

As a planar tensile crack propagates through a medium, the split medium opens and a gap is formed by the progressing crack. The size of this gap can be characterized by the crack width which is sometimes termed the crack opening displacement (COD) or the associated crack opening angle (COA) which is related to the COD via the crack length, see Figure 3.

In a brittle material, as the crack opening displacement increases the crack length increases and the work done in propagating the crack is used to create the new crack surface, thus the concept of energy per area as expressed by G_F.

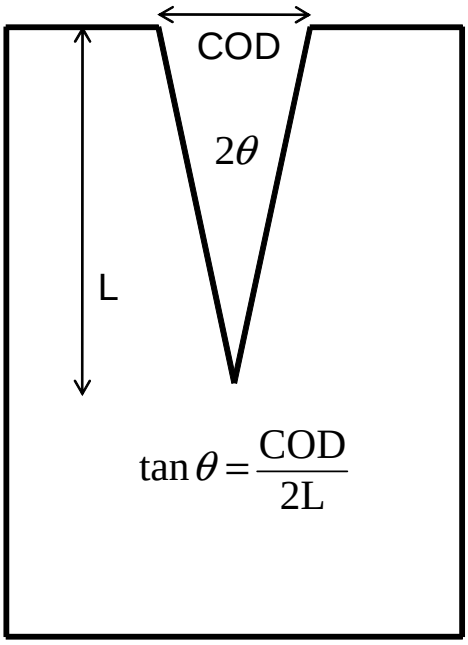

Figure 3 Illustration of crack opening displacement and angle.

The crack width formulation used in the Winfrith (*MAT085) concrete model is based on the work of Wittmann, et al. (1988). Wittmann measured the specific fracture energy, crack opening displacement and maximum load for a large number concrete samples with varying aggregate size, compressive strengths, loading rates, water-to-cement ratios, and test specimen sizes. The aggregate sizes and unconfined compressive strengths are listed here in Table 3, transcribed from Table 2 in Wittmann.

Table 3 Aggregate size and unconfined strengths for tested concretes.

Aggregate Diameter (mm)	Unconfined Compressive Strength (MPa)		
8	40.6	39.0	30.2
16	42.9	37.7	24.4
32	42.2	39.2	28.7

The results of Wittmann's measurements are force versus displacement variations, as idealized in the left most image in Figure 4. The area under this curve is the work done on the specimen. Using a technique based on the *fictitious crack model* the force-displacement data is transformed into stress versus displacement, as idealized in the right most image in Figure 4. The area under this stress-displacement curve is the specific fracture energy G_F.

The maximum tensile stress in the stress-displacement curve is the unconfined tensile strength f_t', since until the stress reaches that value there is no crack propagation. Wittmann uses the unconfined tensile strength[5] and specific fracture energy to develop a nondimensional (normalized) version of the stress versus displacement curve, referred to as the strain softening response, as shown in Figure 5. In this version of the crack softening response, the ordinate break point is selected as 25% of f_t' and the parameter c is given by

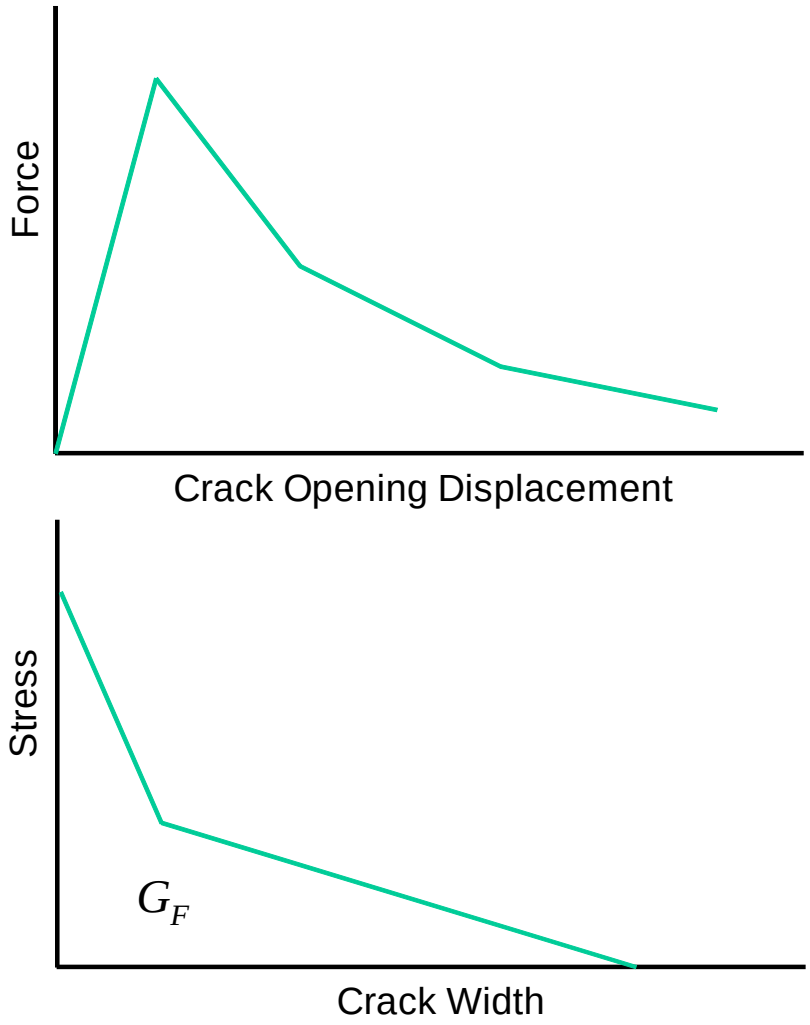

[5] One of the limitations of the Wittmann data is the tensile strengths were not measured, but rather estimated. The estimation method was not described by Wittmann et al.

Figure 4 Measured force versus displacement (left) and corresponding converted stress versus displacement.

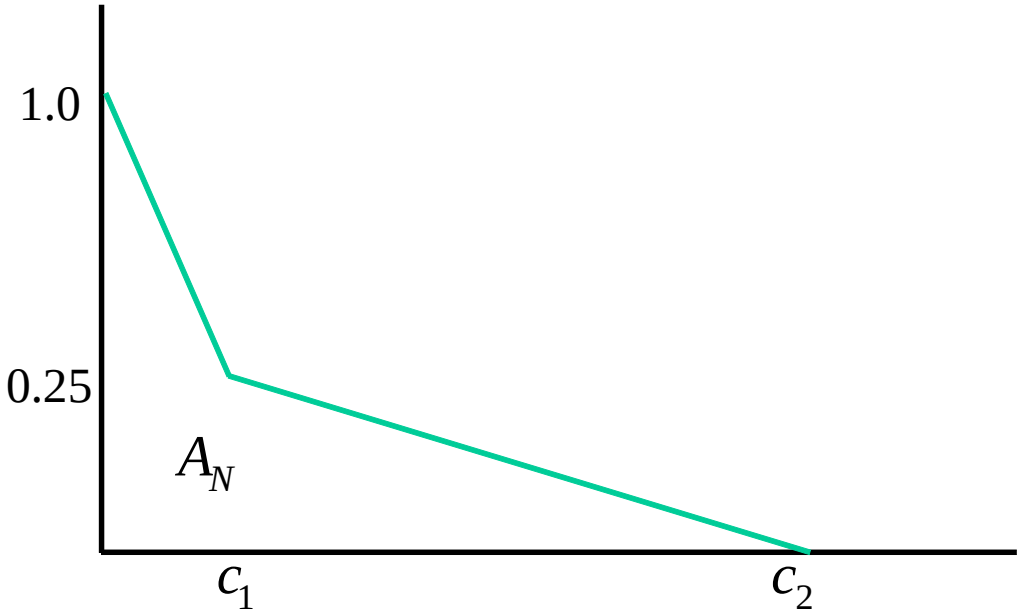

Figure 5 Nondimensional version of the crack strain softening response.

$$c = w\frac{f_t'}{G_F}$$

where w is the crack width.

The area under the normalized strain softening curve must be unity, which leads to the relation

$$A_N = 1 = 0.5\left(c_1 + \frac{c_2}{4}\right)$$

for c_1 and c_2, this is Equation (1) in Wittmann et al. The laboratory data collected by Wittmann et al. is summarized in five normalized strain softening curves in their Figure 14. The five strain softening curves represent variations in: specimen size (ligament length), displacement rate, and the three maximum aggregate sizes of 8, 16, and 32 mm.

Cracking Form with Strain Rates (RATE=0)

Since the two ordinate values of the normalized strain softening curve are always the same, i.e. unity and 0.25, only the two abscissa values change for all of the measured responses. Broadhouse and Attwood (1993) took advantage of this form of the Wittmann et al. data to form

an average strain softening response, by averaging the values of c_1 and c_2 as shown here in Figure 6. NOTE: Figure 3b in Broadhouse and Attwood (1993) shows the value of c_2 as 5.16, but the average of the Wittmann data is 5.14 as shown here in Figure 6.

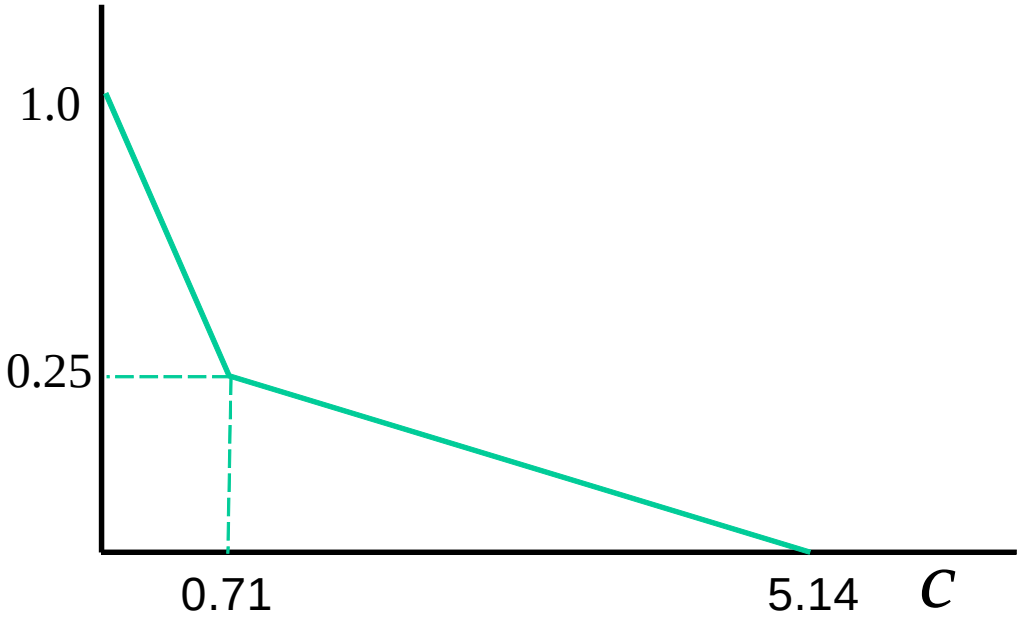

Figure 6 Broadhouse & Attwood average strain softening response.

The average strain softening response, shown in Figure 6, is implemented in the Winfrith concrete model in LS-DYNA as *MAT084, i.e. with strain rate effects RATE=0 and FE is the fracture energy. When the user specifies the specific fracture energy G_F the two crack widths are determined via

$$w_i = c_i \frac{G_F}{f_t'}$$

Where $c_i = 0.71$ or 5.14. The current crack width is determined using the strain normal to the crack surface and a measure of the element size,

$$w = \varepsilon L$$

where L is the cube root of the element volume. As the crack width increases, the tensile stress normal to the crack surface is scaled as per Figure 6.

NOTE: The user specified aggregate size is used to determine the shear stress capacity across the cracking surface (friction), and does not affect the strain softening directly.

Cracking Form without Strain Rates (RATE=1)

The no strain rate form of the Winfrith concrete model (*MAT085), selected via RATE=1, uses the crack width at which the tensile normal stress across the crack is zero, as the user input for the parameter FE.

For this form of tensile cracking, the strain softening response is simplified to a straight line, as illustrated in Figure 7. The area under this curve is still the specific fracture energy. Thus if the user knows the specific fracture energy G_F they can easily compute the crack width at zero stress via

$$w = \frac{2G_F}{f_t'}$$

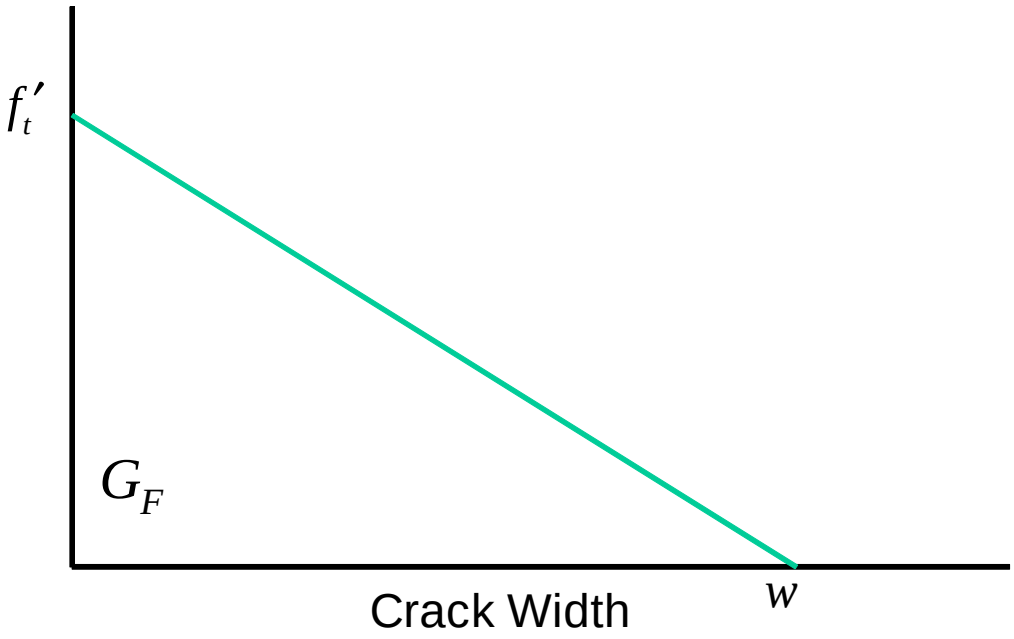

Figure 7 Linear strain softening response for no rate *MAT085.

CEB Recommendations

The CEB (1993) provides tables of specific fracture energies for several unconfined compressive strength concretes with differing maximum aggregate sizes; also provided are mean tensile strengths for the same range of concrete compressive strengths. For a 60 MPa unconfined compressive strength concrete, the unconfined tensile strength is 4.6 MPa and the following crack widths, i.e. w, w_1 and w_2, given here in Table 4, are computed for the given aggregate size and specific fracture energy.

NOTE: the crack widths for the linear strain softening response, i.e. w for *MAT085, lie between the corresponding bilinear crack width values, i.e. w_1 and w_2 for *MAT084.

Table 4 Crack widths for a 60 MPa unconfined compressive strength concrete.

Max Aggregate Diameter (mm)	G_F (N/m)	w (mm)	w_1 (mm)	w_2 (mm)
8	95	0.041	0.015	0.107
16	115	0.050	0.018	0.129
32	145	0.063	0.022	0.163

Simple Loading Cases – Verification

In this section a few simple loading cases are simulated and the results compared with expected results: either as specified via input quantities or determined from the analytical form of the Winfrith concrete material model.

The input for the Winfrith material model, using the unit system of grams-millimeters-milliseconds (CONM=-3), is

```
$                                MPa - mm - msec
*MAT_WINFRITH_CONCRETE
$#     mid        ro        tm        pr       ucs       uts        fe     asize
        85  1.60e-3  33536.79      0.18     41.36     2.068     0.127     9.779
$#       e        ys        eh    uelong      rate      conm      conl      cont
                                                1.0      -3.0     0.000     0.000
$#    eps1      eps2      eps3      eps4      eps5      eps6      eps7      eps8
     0.000     0.000     0.000     0.000     0.000     0.000     0.000     0.000
$#      p1        p2        p3        p4        p5        p6        p7        p8
     0.000     0.000     0.000     0.000     0.000     0.000     0.000     0.000
```

This is a 41 MPa (6 ksi) unconfined compression strength concrete with a strength ratio of 0.05 $(= f_t'/ f_c')$, an approximate density of 2400 kg/m^3 (150 pcf), containing aggregate of 9.7 mm (0.385 inch) diameter, and specified to have a crack width dimension of 0.127 mm (0.005 inch) when no tensile force exists (controls the tensile softening response). Unless otherwise noted, the strain rate effects (RATE=1) are turned off.

Hydrostatic Compression Test

As described in the previously, the Winfrith concrete model provides the user with a default pressure versus natural volume strain definition. A single solid hexahedra element, a unit cube, was used to verify the Winfrith default pressure versus volume strain response by prescribing uniform displacements on all side of the unit cube and plotting the resulting pressure versus natural volume strain, as shown in Figure 8. The solid line represents the continuous results from the LS-DYNA unit cube simulation and the filled squares are the Winfrith default pressure versus volume strain data from Table 1 for an unconfined compressive strength of 41 MPa and

bulk modulus of 17.5 GPa. As can be seen in Figure 8, the LS-DYNA results reproduce the Winfrith default pressure versus volume strain data.

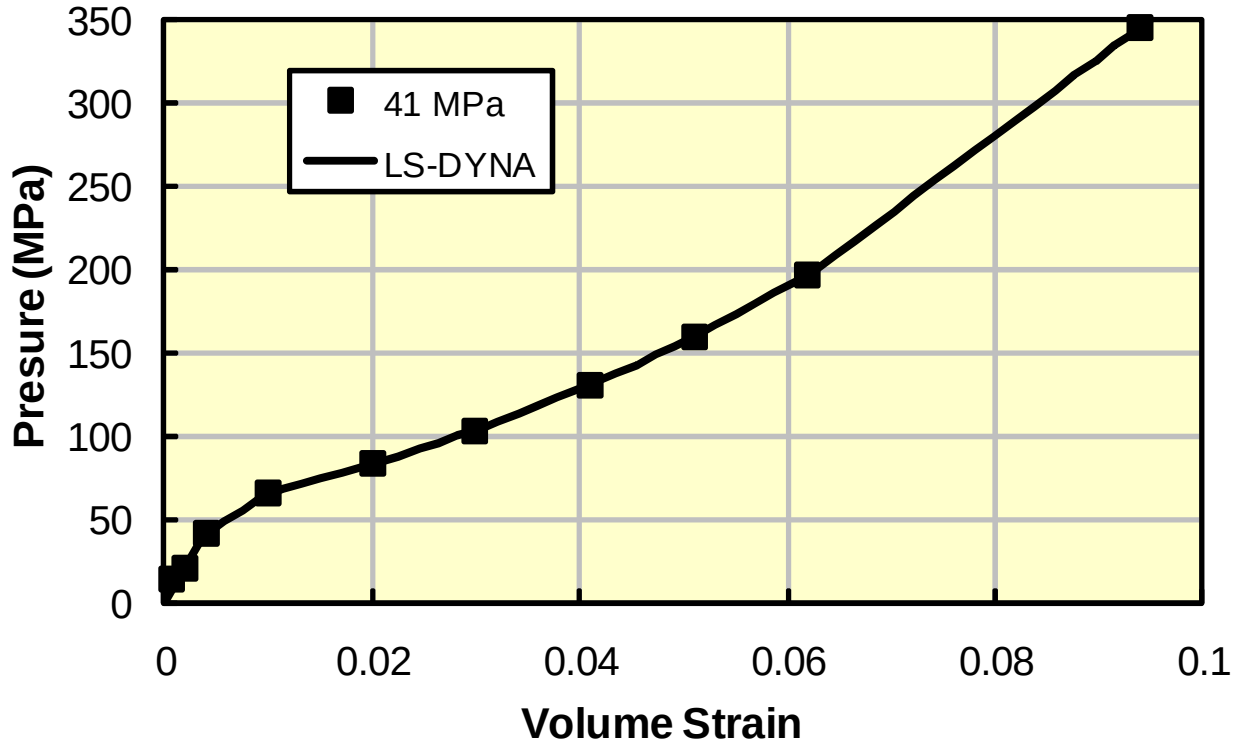

Figure 8 Verification of pressure versus volume strain for an f_c' =41 MPa concrete.

While such unit cube sample problems are easy to construct, it is recommended that more complex specimen geometries also be exercised. In particular, geometries with non-uniform mesh discretization to allow for the possibility of mesh sensitivities such as occur in softening or cracking response. Such a non-uniformly meshed right circular cylinder is shown in Figure 9. The cylinder has a diameter and height of 400 millimeters. Only half the cylinder is shown to indicating the 10 elements selected for sampling the various required stress and strain quantities.

Figure 10 shows that the LS-DYNA cylinder averaged pressure versus natural volume strain results also reproduce the Winfrith default pressure versus volume strain data, as expected.

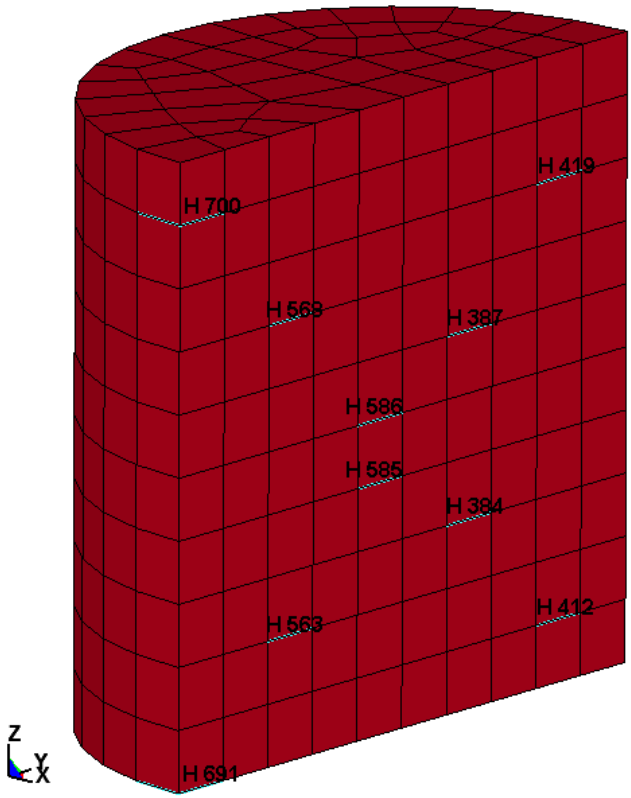

Figure 9 Non-uniformly meshed right circular cylinder.

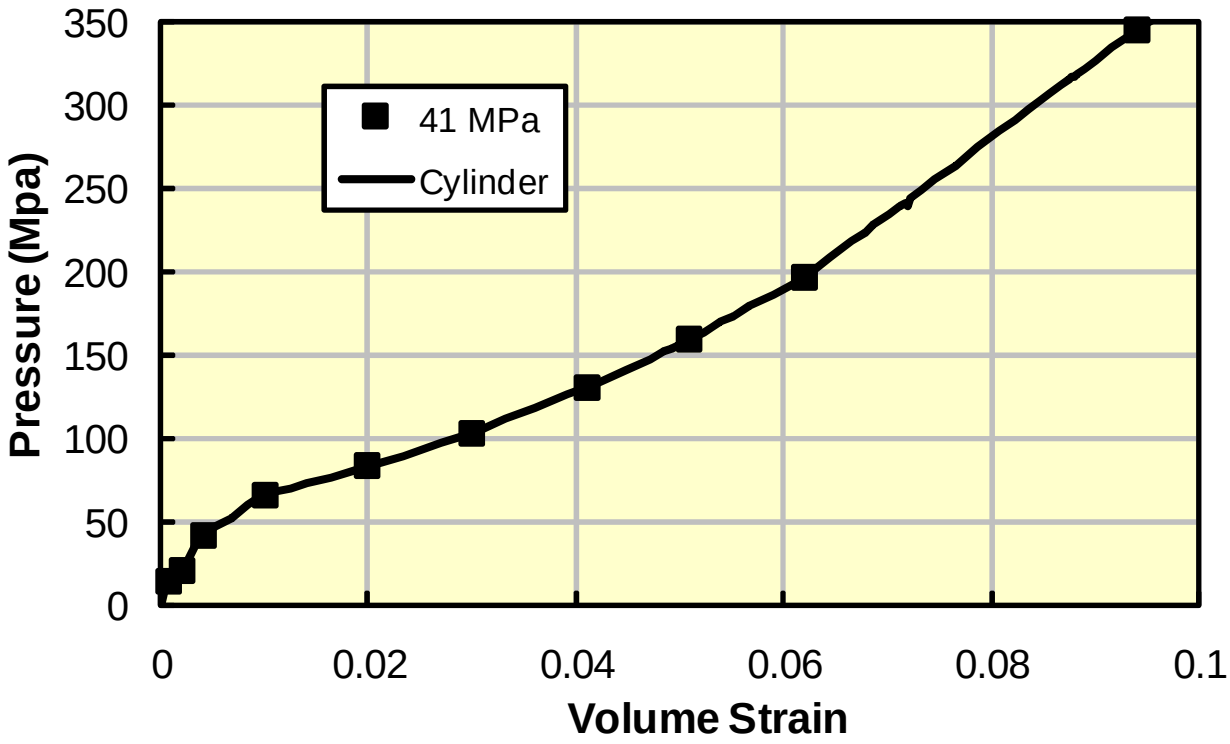

Figure 10 Verification of pressure versus volume strain for an f_c' =41 MPa concrete using the non-uniformly meshed cylinder.

Unconfined Compression Test

An unconfined compression test (UCT), see Figure 11, consists of a prescribed axial load on an otherwise unconstrained specimen. The laboratory version of this test is used to determine the unconfined compression strength f_c'.

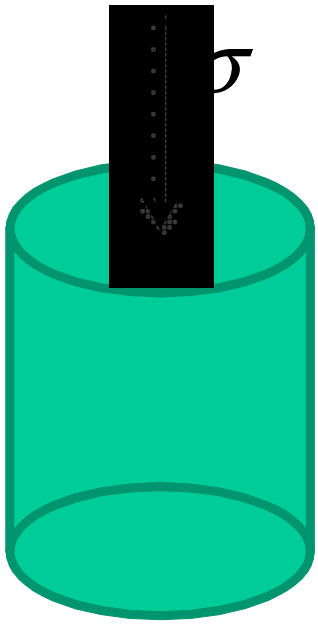

Figure 11 Schematic of an unconfined compression test.

Single Hexahedra

A single solid hexahedra element, a unit cube, was used to verify the prescribed unconfined compressive strength of 41.2 MPa. The boundary conditions consist of prescribed axial displacement on the top of the unit cube with the lateral surfaces traction free; the bottom surface is constrained against only axial motion.

Since this simulation is in a state of uniaxial stress, the axial strain at failure is given by

$$\varepsilon_{fail} = \frac{f_c'}{E} = \frac{41.2}{33536.8} = 1.22 \times 10^{-3} \tag{20}$$

The top surface was prescribed to move -0.002 mm at 1.5 ms (low strain rate of 1.3/second) and then remain constant, see Figure 12. For the unit cube specimen, this maximum displacement corresponds to an engineering axial strain of -0.002, which exceeds the failure strain. By exceeding the failure strain, via prescribed displacement, an assessment of possible strain softening in compression can be made.

Figure 13 shows the resulting axial stress versus axial strain for the unit cube unconfined compression test simulation; the geomechanics sign convention of compression positive is used in this figure. As expected, the unit cube does reach a maximum stress of 41.2 MPa at a strain of 0.00122. After this failure point the axial stress remains constant and the axial strain continues to increase to the prescribed 0.002 value. There is no indication of strain softening in this simulation.

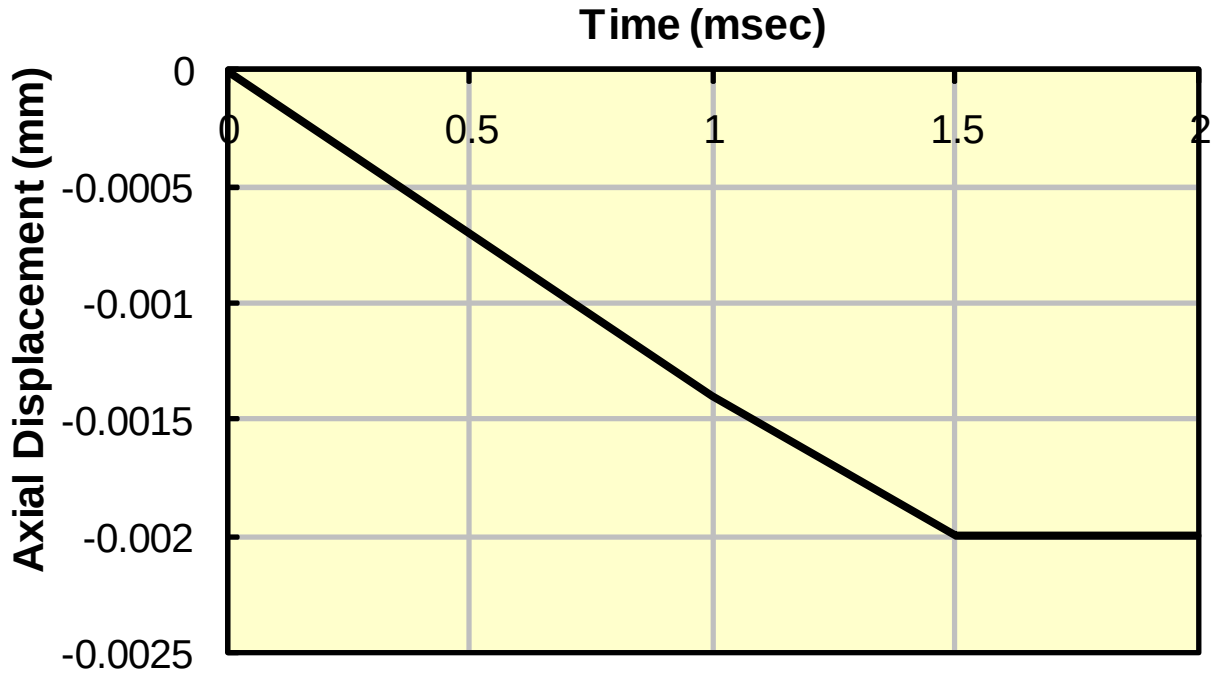

Figure 12 Prescribed axial displacement for top surface in unconfined compression simulation.

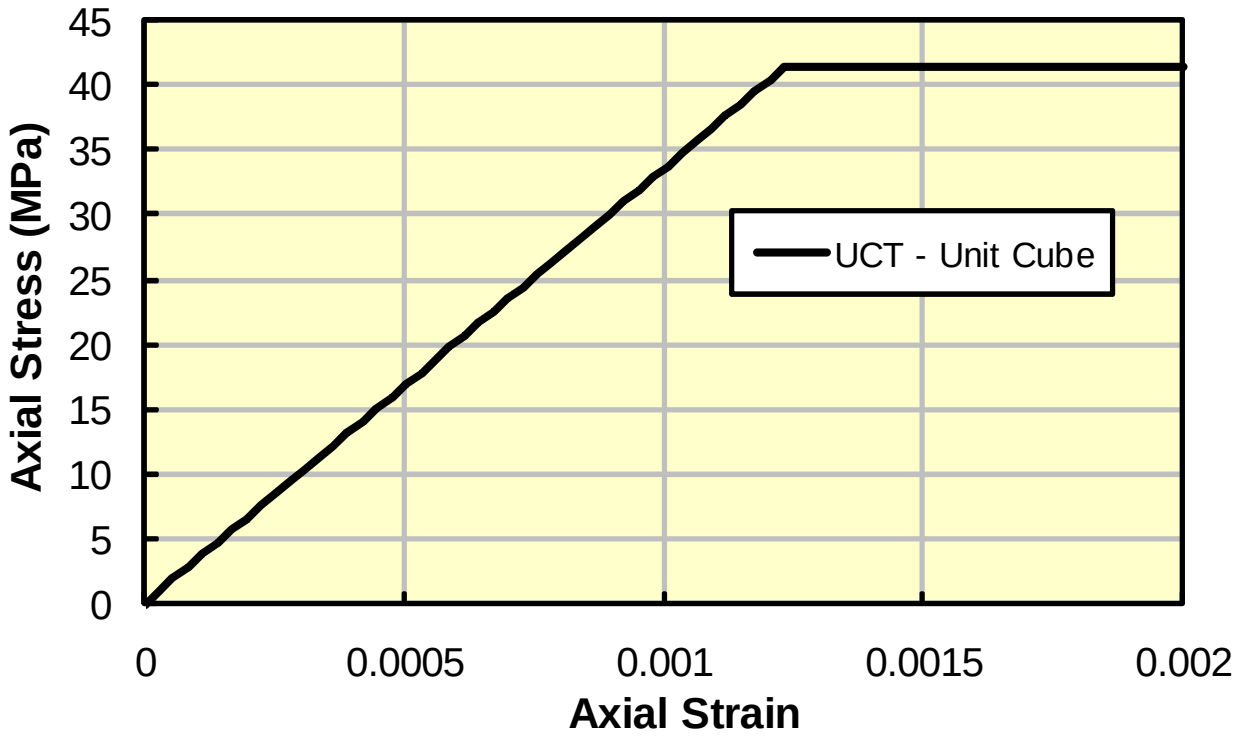

Figure 13 Axial stress versus axial strain for unit cube UCT simulation.

Figure 14 shows the axial and lateral strain histories from the unit cube unconfined compression test simulation. In this figure there is a change in the slope of the lateral strain at about 0.9 ms which corresponds to the time when the axial failure strain of 0.00122 is attained. At this point two orthogonal crack planes are introduced by the Winfrith concrete model, as shown in Figure 15. These orthogonal crack planes are oriented parallel to the compression direction. Although the axial strain ceases to increase after 1.5 ms, as prescribed, the lateral strains continue to increase as the lateral momentum imparted to the nodes, via the Poisson effect, continues to move these nodes at a constant lateral velocity, since the element has no stress in the lateral direction; recall the element was traction free on the lateral surface, e.g. zero lateral stress.

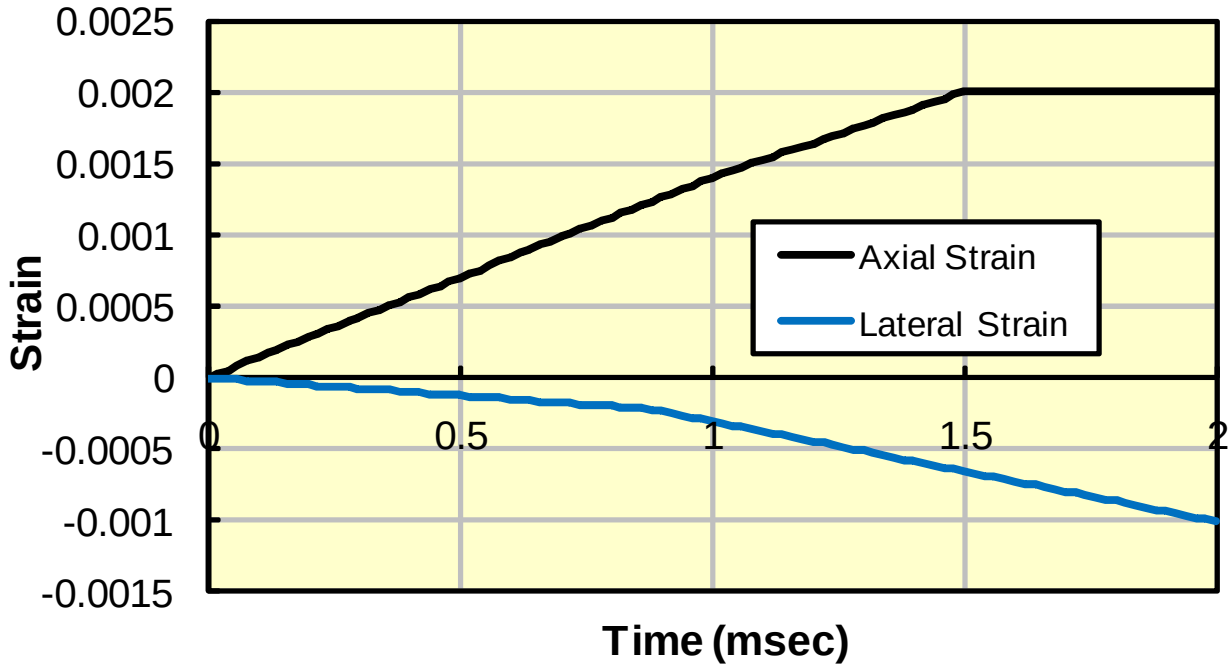

Figure 14 Axial and lateral strain histories for unit cube simulation of an unconfined compression test.

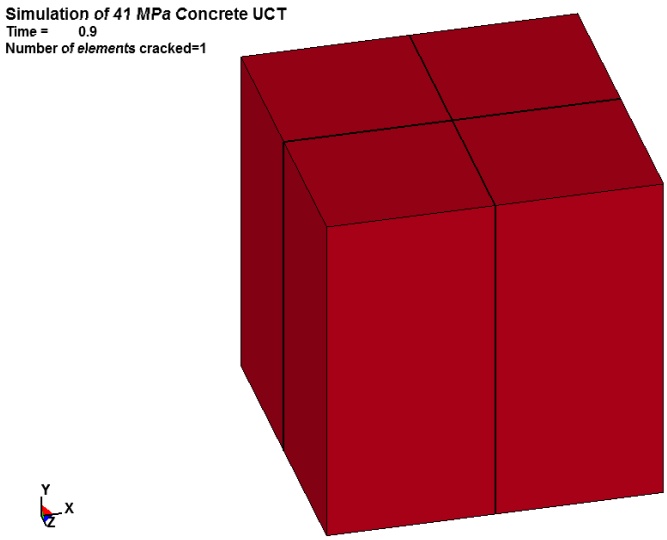

Figure 15 Two orthogonal crack planes introduced in the unit cube when the unconfined compressive strength is reached.

Non-uniformly Meshed Cylinder

The same unconfined compression test simulation is performed using the non-uniformly meshed right circular cylinder. Again the boundary conditions are prescribed displacement of the top surface and traction free lateral surfaces. The top surface displacement is prescribed to move 0.488 mm in 15 ms, for an engineering axial strain of 0.00122, since the cylinder is 400 mm in length. After this compressive failure strain is reached, the top surface continues to a prescribed displacement of 0.8 mm at 20 ms, and then the displacement is held constant. This is a lower strain rate of 0.1/second than used in the unit cube (1.3/second) since that faster strain rate does not approximate quasi-static response in the cylinder, i.e. wave propagation effects will be present.

Figure 16 shows a comparison of the axial stress versus axial strain from the unit cube and the non-uniformly meshed cylinder. As expected, the axial stress strain response for the unit cube and cylinder are nearly identical. For the cylinder, an average of the axial stress and strain from the 10 selected (refer back to Figure 9) elements was used in constructing the stress-strain response. The amount of *lateral strain* variability in the 10 elements selected from the cylindrical sample is shown in Figure 17.

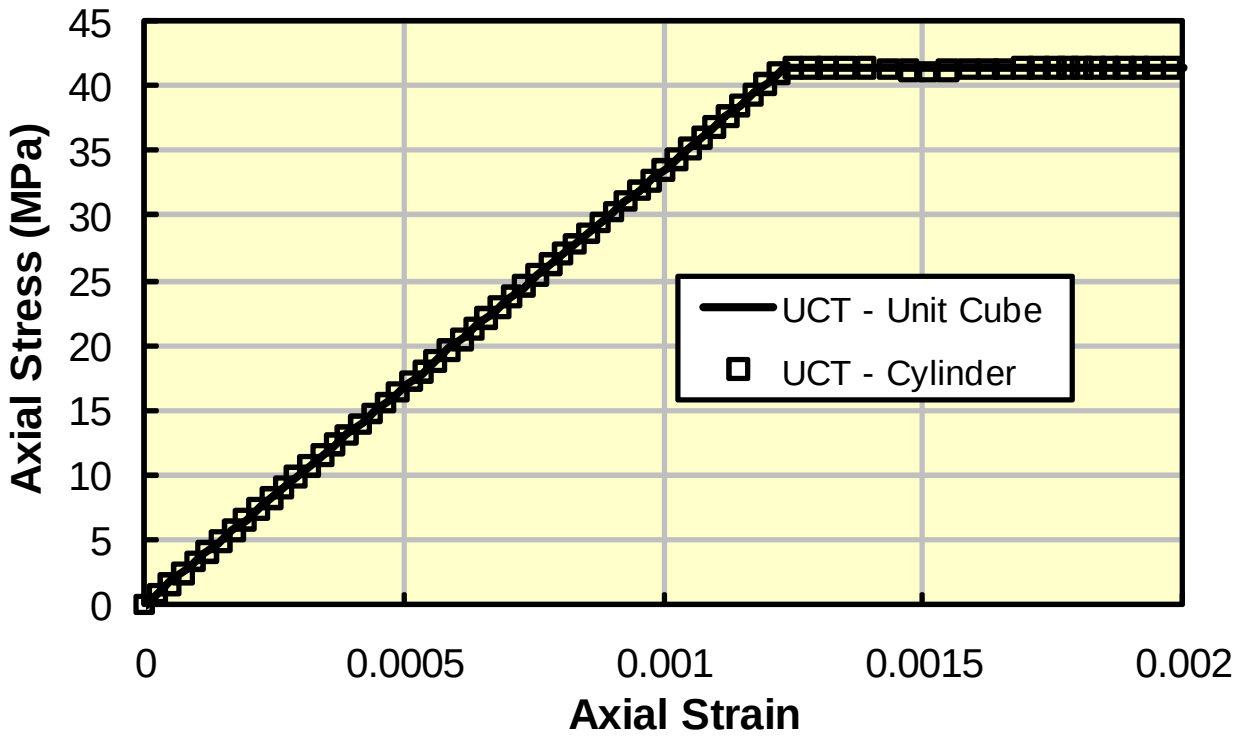

Figure 16 Comparison of unit cube and cylinder axial stress versus axial strain for UCT simulation.

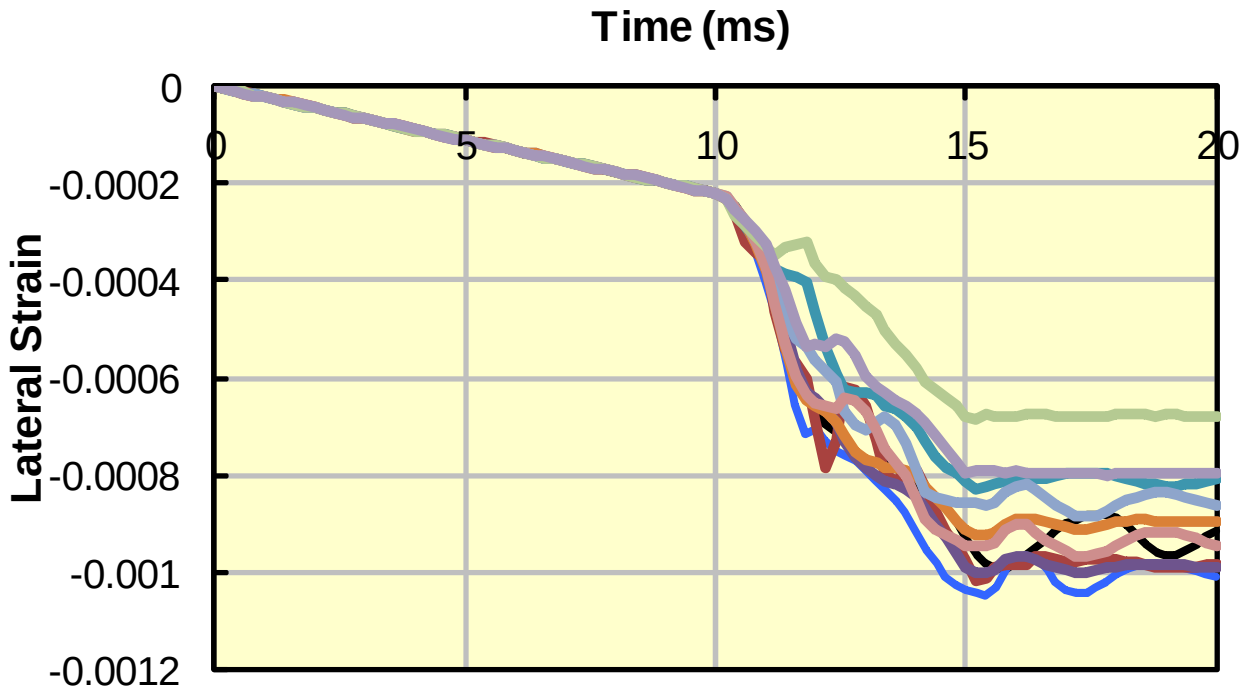

Figure 17 Illustration of variability in the lateral strains for the 10 selected elements of the non-uniformly meshed cylinder.

Figure 18 compares the unit cube and averaged axial and lateral strain histories obtained from the non-uniformly mesh cylinder; again the geomechanics sign convention of compression positive has been used. Note: the lateral strains for the cylinder were obtained by requesting the maximum principal strains from the post-processor. The slight difference in slope during the elastic portion of the simulation is due to the two different strain rates. Of interest is the different response for the lateral strains from the cylinder. These strains remain constant while the top surface displacement is constant. This is in contrast to the unit cube, which due to complete failure, continues to strain in the lateral direction due to the imparted lateral momentum.

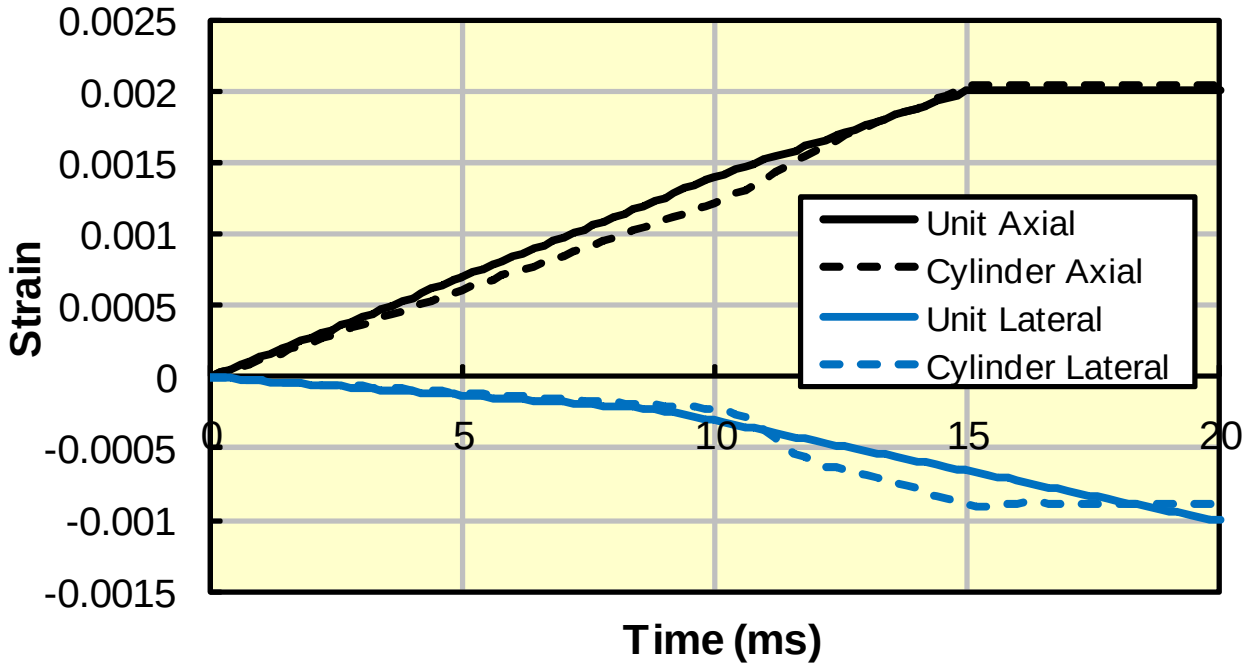

Figure 18 Averaged axial and lateral strain histories from unit cube and non-uniformly meshed cylinder.

The cracking of the non-uniformly meshed cylinder is shown in Figure 19. This figure indicates that not all the elements of the cylinder are cracked, and in particular the cracks do not extend the full height of the cylinder in some axial columns of elements. Since some elements are not fully cracked, the cylinder can resist lateral motion, due to Poisson induced inertial effects, and hence the average lateral strains, shown previously in Figure 18, remain constant when the loading does not increase.

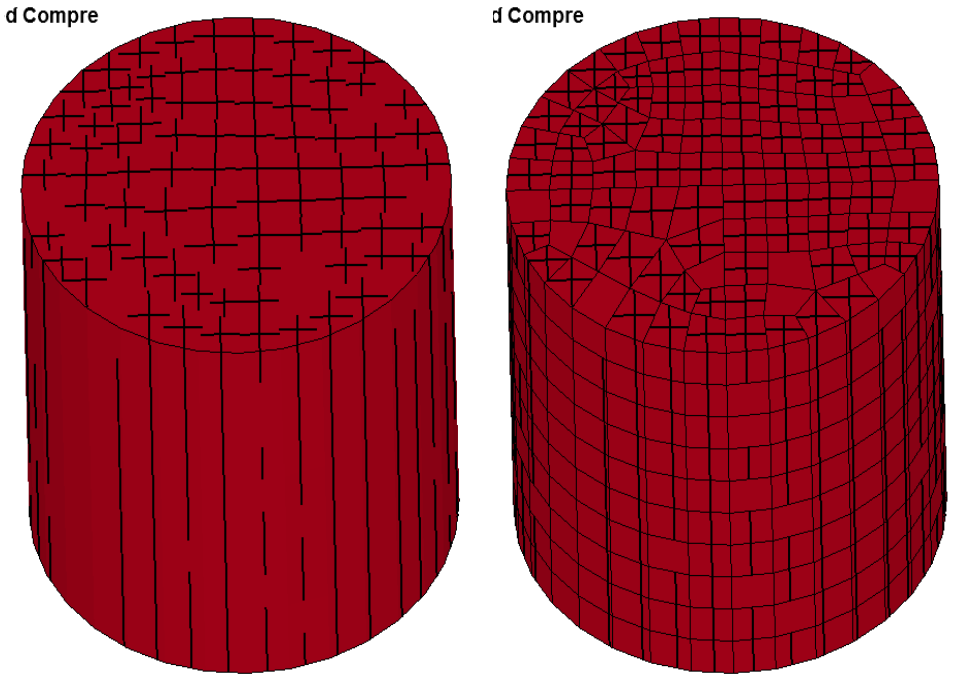

Figure 19 Winfrith crack pattern for non-uniformly meshed cylinder without (left) and with (right) element mesh overlay.

Uniaxial Tension Test

The uniaxial tension test (UTT), see Figure 20, consists of a prescribed axial load on an otherwise unconstrained specimen. The laboratory version of this test is used to determine the unconfined compression strength f_t'.

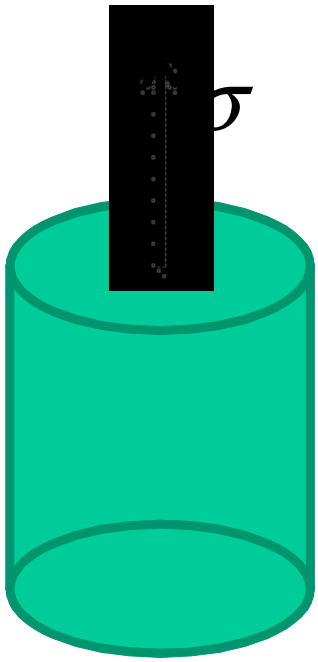

Figure 20 Schematic of an uniaxial tension test.

Single Hexahedra

A single solid hexahedra element, a unit cube, was used to verify the prescribed uniaxial tensile strength of 2.068 MPa. The boundary conditions consist of prescribed axial displacements on the top of the unit cube with the lateral surfaces traction free.

Since this simulation is in a state of uniaxial stress, the axial strain at failure is given by

$$\varepsilon_{fail} = \frac{f_t'}{E} = \frac{2.068}{33536.8} = 6.16\times10^{-5} \tag{21}$$

Although this is the strain at which failure is *initiated*, the failure is not complete until the crack width has attained the prescribed width at which the stress goes to zero, i.e. the Winfrith input parameter FE=0.127 mm.

The top surface was prescribed to move 0.15 mm at 10 ms (low strain rate of 15/second), then remain constant until 20 ms, returning to zero at 30 ms, and then into compression with -0.15 mm displacement at 40 ms, see Figure 21. For the unit cube specimen, this maximum tensile displacement corresponds to an engineering axial strain of 0.15, which exceeds the tensile failure initiation strain and the corresponding crack width (strain) at failure of 0.127 mm. By exceeding the failure initiation and crack width strains, via prescribed displacement, an assessment of the strain softening in tension can be made.

Also, reversing the tensile strain and ‘healing’ the crack allows an assessment of the cracked element’s ability to carry subsequent compression.

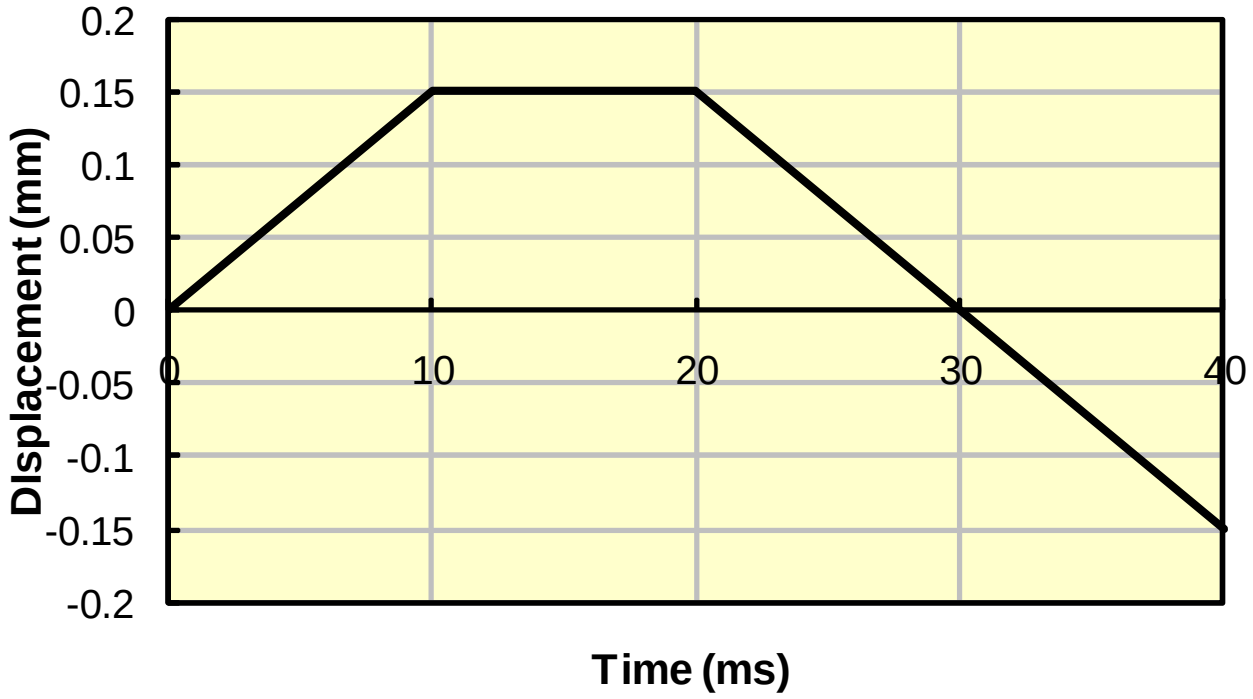

Figure 21 Prescribed axial displacement for top surface in uniaxial tension/compression simulation.

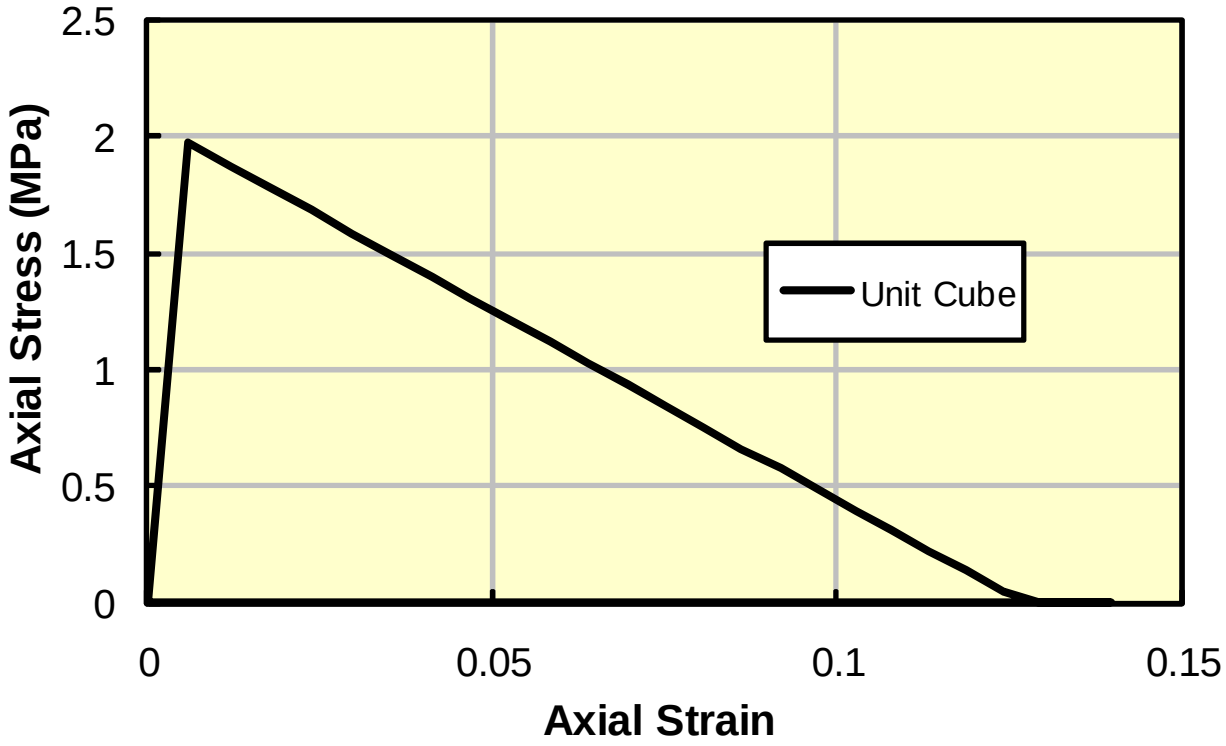

Figure 22 Axial stress versus axial strain for unit cube UTT simulation.

Figure 22 shows the axial stress versus axial strain from the tensile portion of the unit cube uniaxial tensile/compression simulation. As expected, the maximum stress of 2.068 MPa was reached at an axial strain of 1.66×10^{-5}; Figure 22 depicts the maximum stress of 1.97 MPa at a strain of 5.98×10^{-3} as those were the values with the coarse sampling rate of 0.4 ms. The maximum stress then decreases linearly to a strain of 0.127 which corresponds to the Winfrith parameters FE=0.127 mm. The prescribed axial strain then increases to 0.15 before reversing and returning to zero strain.

Next the strain is increased in compression from the zero value at the end of the tensile cycle to a compressive strain of -0.15. The correspond axial stress versus axial strain is shown in Figure 23. The complete axial stress strain cycle is shown in Figure 24.

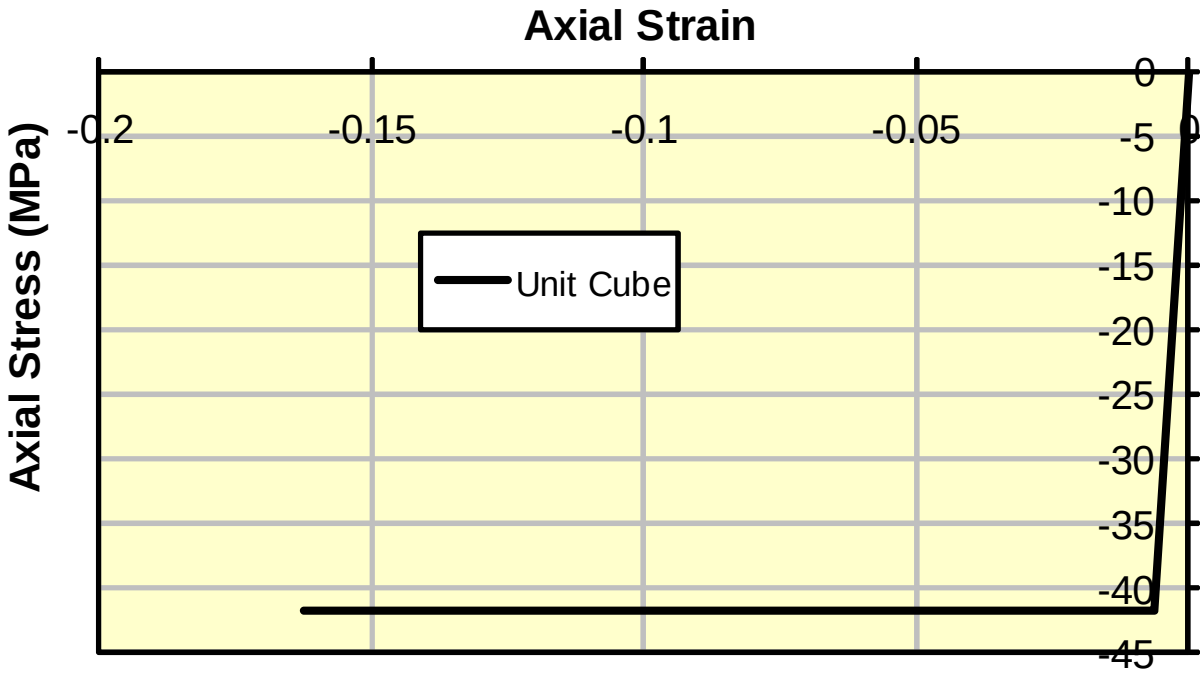

Figure 23 Axial stress versus axial strain for compressive loading following tensile failure.

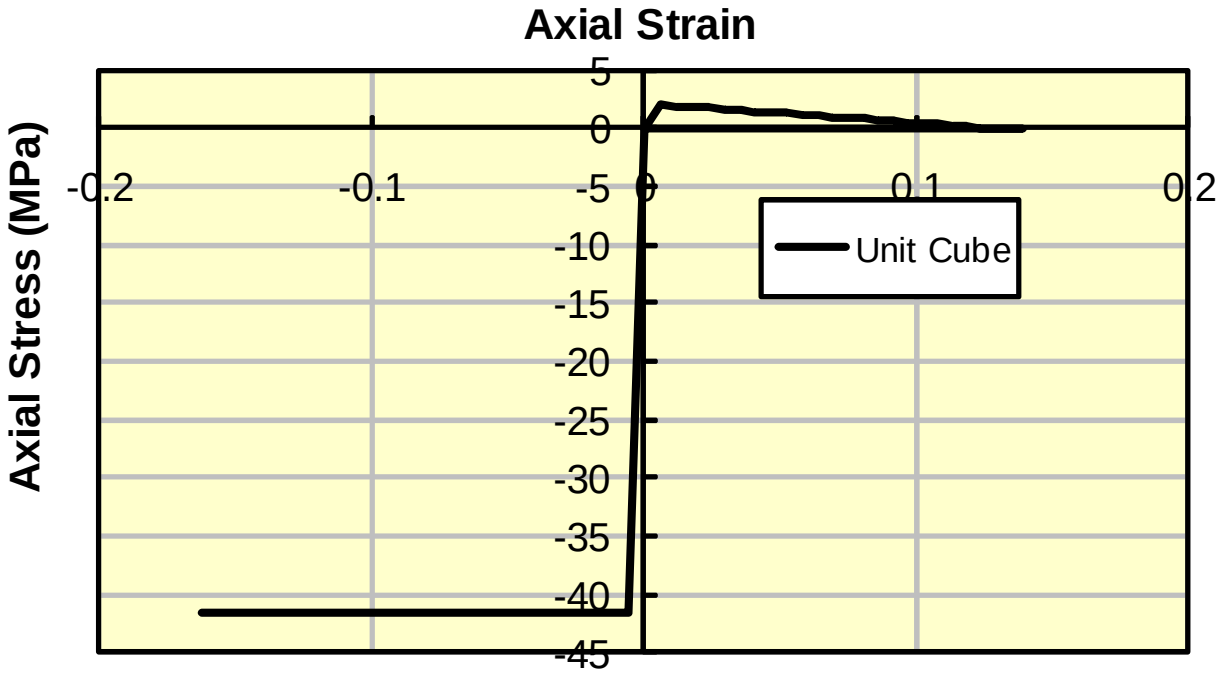

Figure 24 Complete axial stress versus axial strain response for uniaxial tensile and compressive cycle of loading.

Figure 25 shows the single crack plane that develops in the unit cube when the crack width displacement criterion is satisfied, i.e. FE=0127 mm at 9.2 ms. The crack plane is perpendicular to the (vertical) loading direction. Subsequently, at 30.4 ms, in the compression portion of the loading cycle, this horizontal tension crack plane is 'healed' and a pair of orthogonal crack planes develops when the unconfined compression strength is reached.

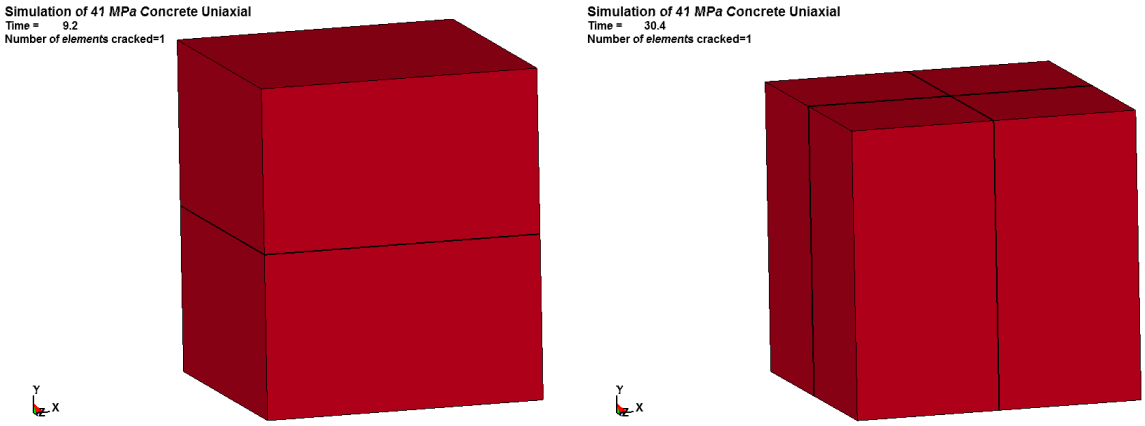

Figure 25 Single tensile crack plane introduced in unit cube when the uniaxial tensile strength is reached (left) and double orthogonal tensile crack planes when compressive strength is reached.

Non-uniformly Meshed Cylinder

The same cyclic uniaxial test simulation is performed using the non-uniformly meshed right circular cylinder. Again the boundary conditions are prescribed displacement of the top surface and traction free lateral surfaces. The top surface displacement is prescribed to move 0.15 mm in 15 ms, for an overall average engineering axial strain of 3.75×10^{-4}, since the cylinder is 400 mm in length. However, since there are 10 elements along the 400 mm cylinder height, the nominal element strain would be $3.75\times10^{-5}\left(=3.75\times10^{-4}/10\right)$. While both of these strains exceed the initial failure strain of 6.16×10^{-5}, the equivalent strain at which the crack stress is zero would be $3.175\times10^{-4}\left(=0.127/400\right)$ for overall specimen average, or $3.175\times10^{-5}\left(=3.175\times10^{-4}/10\right)$ for a nominal element. If the equivalent strain at which the crack stress is zero, localizes in one element, then the strain will be $3.175\times10^{-3}\left(=0.127/400\right)$, i.e. all the displacement will occur in one element.

As with the unit cube, once the top surface reached the prescribed displacement of 0.15 mm at 15 ms, then the displacement is held constant until 20 ms when it is reduced back down to zero. This completes the tension portion of the loading cycle. Next the strain is increased in compression with a top surface moving to -0.55 mm at 40 ms, see Figure 26. The 0.55 mm compressive displacement provides an average compressive strain of 1.375×10^{-3} which exceeds the compressive failure strain of 1.22×10^{-3}, recall Equation (20). Again the intent of the strain

reversal is to make an assessment of the cylinder's ability to carry compression after tensile failure.

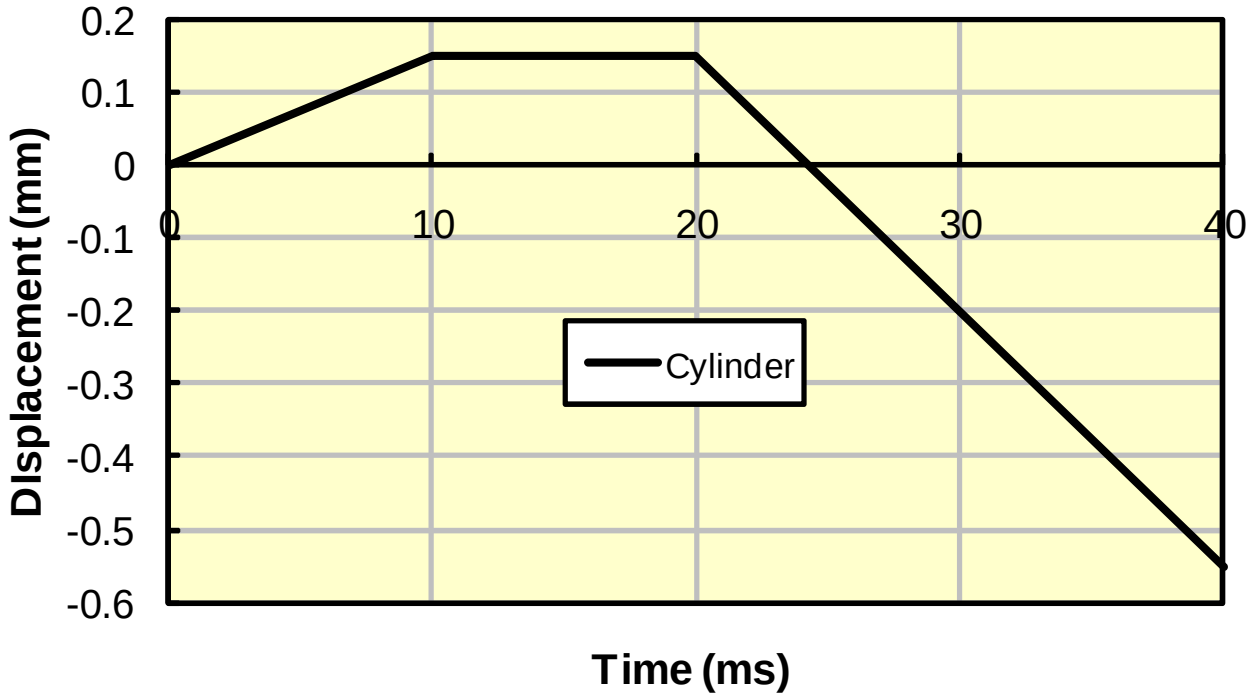

Figure 26 Tension and compression loading cycle for the non-uniformly meshed cylinder.

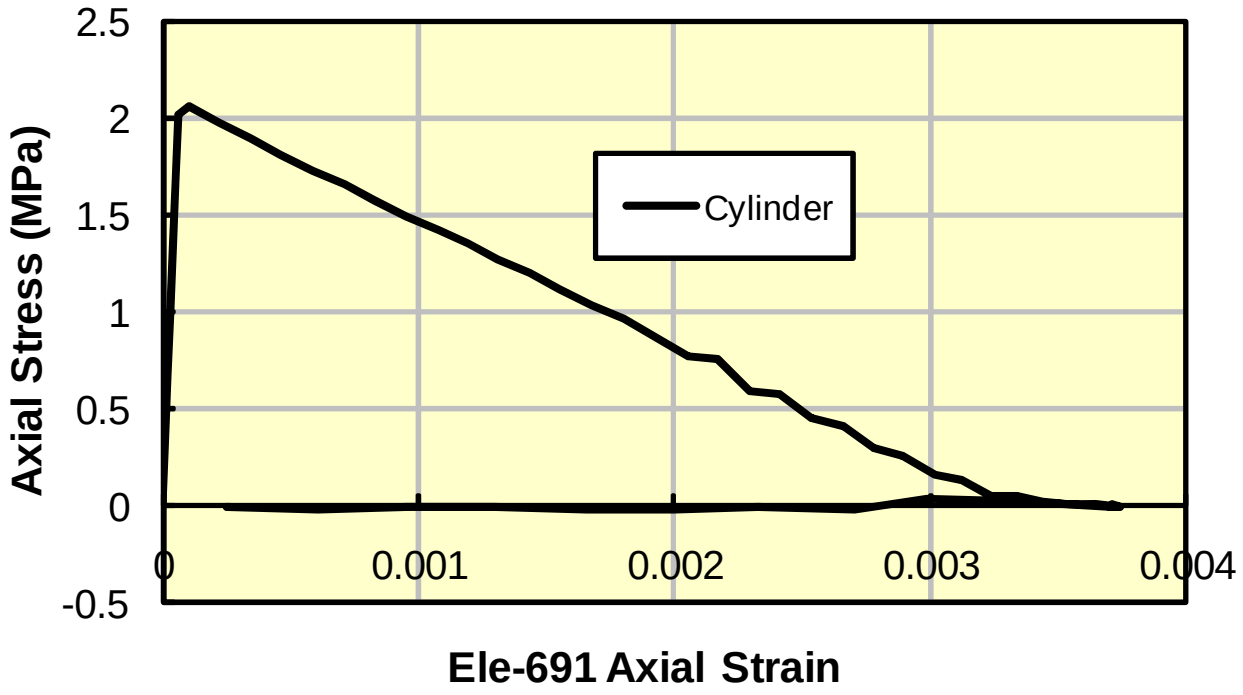

Figure 27 Axial stress versus Element 691 axial strain for cylinder UTT simulation.

Figure 27 shows the axial stress versus axial strain (Element 691) for the non-uniformly meshed cylinder acting under the uniaxial tension portion of the above described loading. The reason for plotting the axial strain for Element 691, rather than the average axial strain, is the displacement localized in the bottom layer of the cylinder's elements, where Element 691 is located. Figure 28 shows the Winfrith model tensile cracks and the location of Element 691. Since the Winfrith model cracks localized in one layer of the cylinder, the other elements in the cylinder had very low strain levels, i.e. up to the initial failure strain (elastic response), and then these low strain levels decreased to zero as the bottom layer of elements in the cylinder accounted for all the overall strain via localization.

Check on the strain to failure for Element 691

$$\text{Volume} = V = 6.086\times10^{4}\ \text{mm}$$
$$L = V^{1/3} = 39.33\ \text{mm}$$
$$w = 0.127\ \text{mm (prescribed)}$$
$$\varepsilon = \frac{w}{L} = \frac{0.127}{39.33} = 3.22\times10^{-3}$$

Next the strain is increased in compression from the zero value at the end of the tensile cycle to a compressive strain of 1.375×10^{-3} which exceeds the compressive failure strain. The correspond axial stress versus axial strain is shown in Figure 29. The complete axial stress strain cycle is shown in Figure 30.

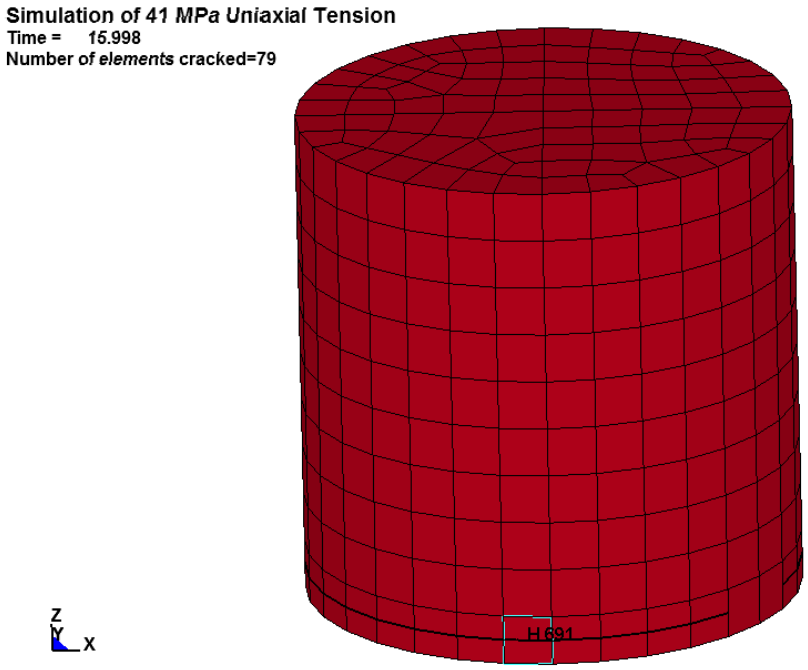

Figure 28 Winfrith model crack pattern at bottom layer of non-uniformly meshed cylinder for UTT simulation.

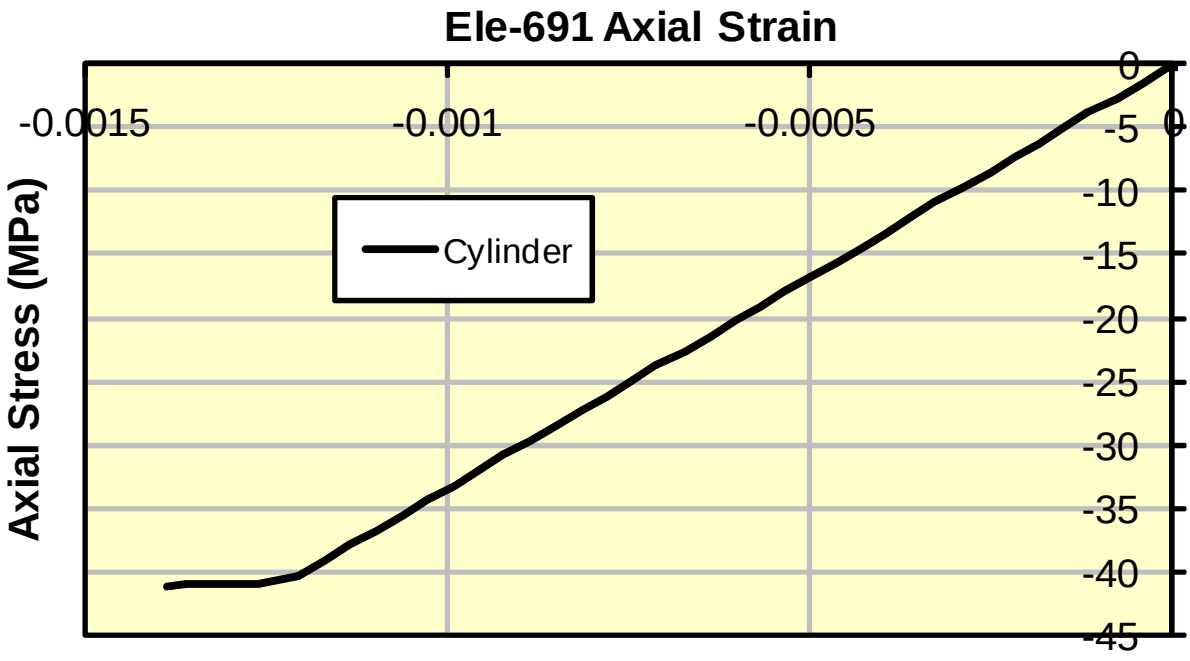

Figure 29 Axial stress versus axial strain for compressive loading following tensile failure in the cylinder model.

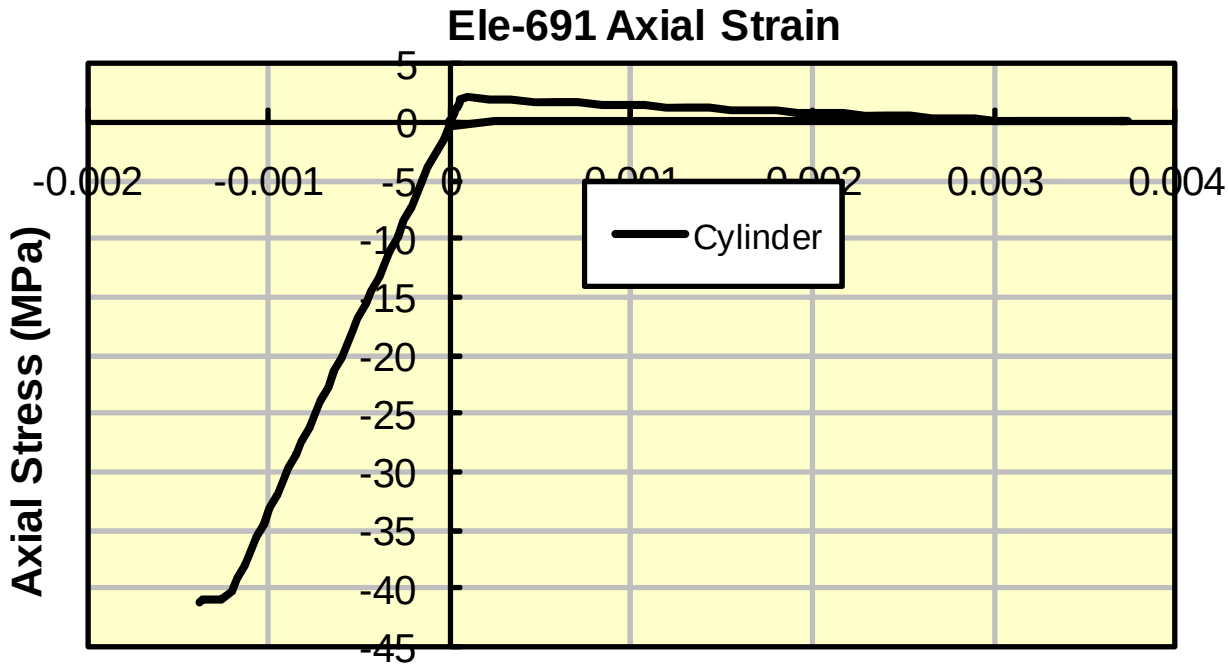

Figure 30 Complete axial stress versus axial strain response for uniaxial tensile and compressive cycle of loading for the non-uniformly meshed cylinder.

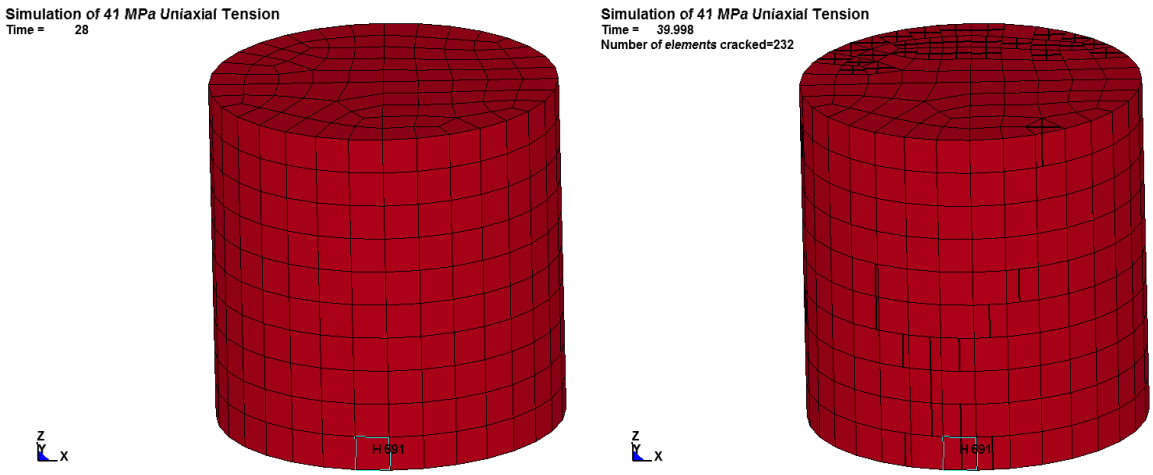

Figure 31 Healed tension crack (left) a 29 ms and appearance of compressive orthogonal crack planes at 40 ms (right).

Figure 31 shows the 'healing' of the Winfrith concrete model tension cracks in the bottom layer of the cylinder at 28 ms. As the compressive portion of the loading cycle continues, pairs of orthogonal tension cracks develop when the compressive failure strain is reached at 40 ms.

It is observed that this crack pattern due to compression after a tension failure cycle is quite different from that obtained for the compression only (unconfined compression tests) simulation, see previous Figure 19.

Simple Loading Cases - Conclusions

The specified compressive and tensile failure strengths and strains were verified via these simple loading cases.

In unconfined compression, the unit cube developed an orthogonal set of Winfrith concrete model crack planes, which are aligned with the compression direction, see Figure 15. It was noted that there is no strain softening after the compression failure occurs. The unconfined compression strength was maintained while the axial and lateral strains increased, i.e. elastic perfectly plastic behavior. While behavior similar to the unit cube was observed for the non-uniformly mesh cylinder, Winfrith concrete model crack planes that develop did not occur in all elements comprising the cylinder. This indicates a mesh size sensitivity.

In the uniaxial tension and compression cyclic loading, the unit cube developed a single Winfrith concrete model tensile crack plane perpendicular to the tensile loading direction. During the subsequent compression portion of the cyclic loading, the tensile crack is healed, the unit cube carries compression until the compressive failure strain is reached when the orthogonal set of Winfrith concrete model crack planes, aligned with the compression direction, develop.

The corresponding behavior for the non-uniformly meshed cylinder demonstrated an apparent lack of strain softening regularization as the Winfrith concrete model tensile crack plane developed only in the bottom layer of elements, and not all those elements were cracked. Further studies of this apparent lack of regularization are recommended, e.g. a rod of solid elements with varying dimensions under tensile loading can be used to assess if the tensile strain always localizes in the smallest element. During the compressive portion of the cyclic loading, the tensile cracks were again ‘healed,’ and subsequently orthogonal pairs of Winfrith concrete model crack planes developed when the compressive failure strain was reached. Oddly, the Winfrith concrete model crack pattern for this compressive loading is quite different than the corresponding crack pattern for the unconfined compression only simulation.

Extra History Variables

Based on the notes from
Richard Stuart & Conrad Izatt of ARUP
and
Jim Day of LSTC
http://ftp.lstc.com/anonymous/outgoing/jday/concrete/mat84_winfrith

Extra	Description		Notes

Variable			
1	Crack Indicators	crakmax	Crack Flag (0=uncracked; 1,2, or 3=cracked)
2		dameng	Crack opening damage variable (mat 84 only)
3		cd1	Crack opening strain in direction 1 (mat 84 only)
4		cd2	Crack opening strain in direction 2 (mat 84 only)
5		cd3	Crack opening strain in direction 3 (mat 84 only)
6	Concrete stresses	σ_x	
7		σ_y	
8		σ_z	
9		τ_{xy}	
10		τ_{yz}	
11		τ_{zx}	
12	Reinforcement stresses	σ_x / σ_A	x, y and z are global directions, if option 1 card is used. A and B depend on layer orientation, if option 2 card is used.
13		σ_y / σ_B	
14		σ_z	
15	Reinforcement ratios	XR / RQA	XR, YR and ZR are reinforcement ratios in global directions, if option 1 card is used. RQA and RQB are reinforcement ratios in A and B directions, if option 2 card is used.
16		YR / RQB	
17		ZR	
18	Crack vector directions	x_{crack_1}	[x y z] is a unit vector normal to the plane of the crack. Crack plane passes through the centre of the element.
19		x_{crack_2}	
20		x_{crack_3}	
21		y_{crack_1}	
22		y_{crack_2}	
23		y_{crack_3}	
24		z_{crack_1}	
25		z_{crack_2}	
26		z_{crack_3}	
27	Principal concrete stresses	sf1	
28		sf2	
29		sf3	
30	Crack Extension	ef1	extension in 1st crack direction and two orthogonal directions
31		ef2	
32		ef3	
33	Plastic strains in reinforcement	ε_{px} / ε_{pa}	Plastic strains in reinforcement in x, y and z global directions, if option 1 card is used. Plastic strains in reinforcement in A and B directions, if option 2 card is used.
34		ε_{py} / ε_{pb}	
35		ε_{pz}	
36	Concrete Crack Indicators	crack_1	1 = cracked, i.e. on softening part of curve. 2 = crack has closed up 3 = fully cracked
37		crack_2	
38		crack_3	
39	Concrete Strains	eps1	
40		eps2	
41		eps3	
42		eps4	
43		eps5	
44		eps6	
45		ex1	set equal to ef1, ef2, ef3, resp. if tensile
46		ex2	
47		ex3	
48		tc1	time that 1st, 2nd, and 3rd cracks initiate

49		tc2	
50		tc3	
51		epv	volumetric yield strain
52		nj	Counter for number of points if pressure-volume?
53		sv	Volume Strain
54		td1	Crack opening history
55		td2	
56		td3	

Set *DATABASE_EXTENT_BINARY parameter NEIPH=56 and post process using LS-PrePost under Fringe > Misc > History Variables 1-56

Graphical Crack and AEA_CRACK Text Files

The LS-DYNA keyword *DATABASE_BINARY_D3CRACK can be used to specify the frequency for writing the graphical crack file indicated on the execution line by the parameter *q=crack_filename*. Unfortunately, the only acceptable value of the frequency is the same frequency used to write the d3plot database, i.e. *DATABASE_BINARY_D3PLOT, as apparently the information in the d3plot file is needed to display the additional information in the graphical crack file.

To display the graphical cracks, first open the d3plot files and then open the graphical crack file via the LS-PrePost Open > Others> Crack File. Step through the simulation to view cracks as they form. Under the *Post Processing* icon there is a *Settings* icon, check the radio button for *Concrete Crack Width*. By adjusting the number in the *minimum crack width* widow, the cracks with smaller widths can be made to disappear. As noted below, the crack widths are apparently in meters and independent of the user specified input length units.

LS-DYNA also generates a text based crack information file named `aea_crack` . This text file is written with the frequency specified via the keyword *DATABASE_BINARY_D3CRACK. NOTE: if the graphical crack file is omitted, i.e. no *q*= on the execution line, then the frequency specified via the *DATABASE_BINARY_D3CRACK will be used to write the text based crack file and thus may differ from the frequency specified via *DATABASE_BINARY_D3PLOT.

Sample `aea_crack` output:

```
 time =  0.190E+01   number of cracked elements =       3
 elements with cracks > 0.1mm wide are printed
element state                crack widths
   1101 3 0 0       0.201E-03  -0.426E-06  -0.133E-04
   1300 3 0 0       0.202E-03   0.723E-05  -0.248E-04
   1301 3 0 0       0.197E-03  -0.774E-06  -0.125E-04

 time =  0.190E+01   tensile damage energy
 part ID      non-crack    crack       total
    1        0.0000E+00  0.0000E+00  0.0000E+00
 total       0.0000E+00  0.0000E+00  0.0000E+00
```

The current simulation time and total number of cracked elements are indicated on the first line. Although the text “>0.1mm” is hardwired into the format statement, the Winfrith model internal units are kilograms-meters-seconds, so the crack lengths are provided in meters and thus independent of the user’s input length units. The next lines list the element numbers of the cracked elements, the ‘crack status’, and crack widths in the three ordinal directions.

The crack status is an integer 0-3 with the following meaning (I think):
0 = Uncracked.
1 = Cracked, but still on strain softening curve (still taking some tensile stress).

2 = Cracked, but crack is closed (i.e. can take compressive stress).
3 = Cracked fully (i.e. crack open and zero tensile stress).

Since cracks smaller than 0.1 mm are not printed to the `aea_crack` file, the most common crack status indicator is the number 3.

NOTE: When the strain rate form of the Winfrith concrete model (MAT084) is used, the tensile damage energies are negative values, else when MAT085 is used, the values always appear to be zero.

The information in the `aea_crack` file is also available via the Extra History Variables and thus can be visualized via LS-PrePost using the afore mentioned Fringe >Misc > History Variables. Perhaps one item that could be added to LS-PrePost, from the ASCII `aea_crack` file is a histogram of the crack widths at a given time. Figure 32 shows a sample of such a crack width histogram

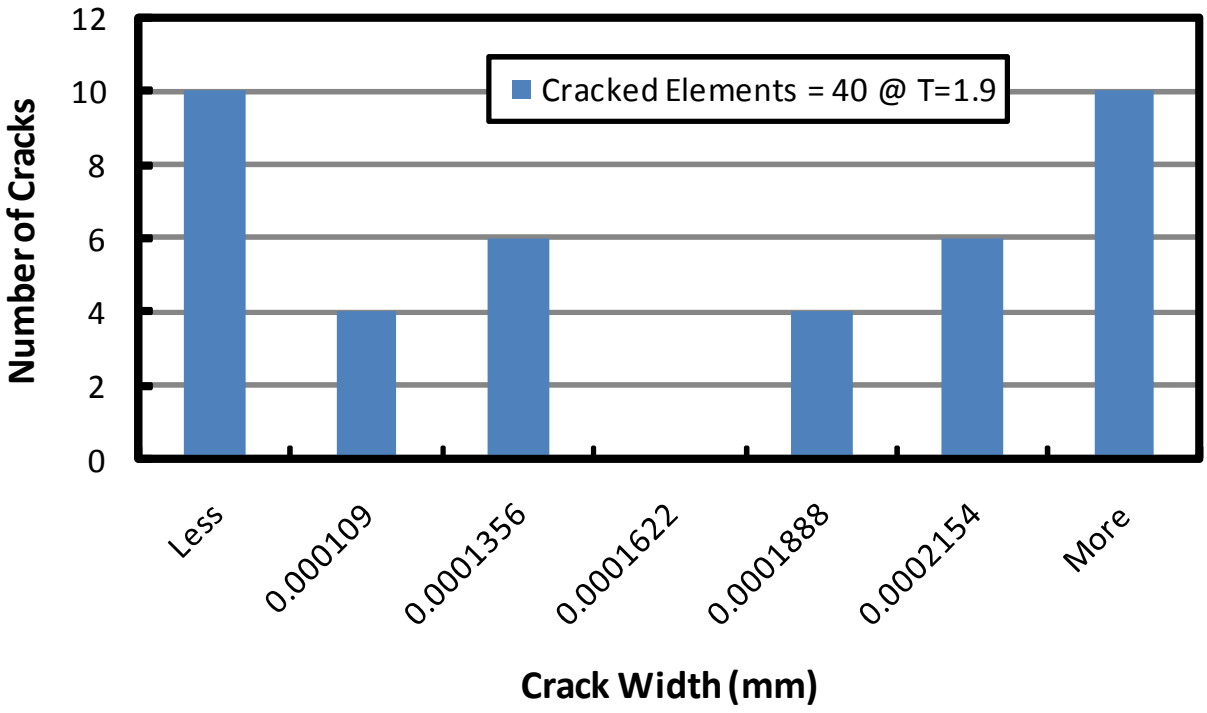

Figure 32 Example of a crack width histogram obtained from the `aea_crack` file.

In this case, the `aea_crack` file a T=1.9 reported there were 40 cracked elements and then proceeded to list the 30 elements with crack widths greater than 0.1 mm (1.0E-4 m).

Acknowledgement

The help and guidance of Richard Sturt and Conrad Izatt, both of ARUP UK, is most greatly appreciated in navigating many aspects of the Winfrith concrete model.

References

Balmer, G.G. (1949) “Shearing strength of concrete under high triaxial stress - computation of Nohrs envelope as a curve,” United States Department of the Interior. Bureau of Reclamation. Structural Research Laboratory. Report No.SP-23, page 13.

Broadhouse, B.J. and G.J. Attwood (1993), “Finite Element Analysis of the Impact Response of Reinforced Concrete Structures using DYNA3D.” Proceedings of Structural Mechanics in Reactor Technology (SMiRT) 12, University of Stuttgart Germany Elsevier Science Publishing.

Kupfer, H., Hilsdorf, H.K. and Rosch, H. (1969) “Behaviour of Concrete under Biaxial Stresses,” *Proceedings of the American Concrete Institute*, Volume 66, pages 656-666.

Kupfer, H. and Gerstle, K. (1973) “Behaviour of Concrete under Biaxial Stress,” *Journal of the Engineering Mechanics Division*, American Society of Civil Engineers, Volume 99, pages 852-866.

Ottosen, N.S., (1977) “A Failure Criterion for Concrete,” *Journal of the Engineering Mechanics Division*, Volume 103, Number 4, July/August, pages 527-535.

Richart, F.E., Braendtzaeg, A., and Brown, R.L. (1928) “A Study of the Failure of Concrete under Combined Compressive Stress,” University of Illinois. Engineering Experimental Station. Bulletin Number 185, page 103.

Malvern, L.E. (1969), *Introduction to the Mechanics of a Continuous Medium*, Prentice-Hall, Englewood Cliffs, NJ.

Spiegel, M.R., (1968) *Schaum's Outline of Mathematical Handbook of Formulas and Tables*, McGraw-Hill Inc., New York, NY.

Comite Euro-International du Beton, *CEB-FIP model code 1990*, Redwood Books, Trowbridge, Wiltshire, UK, 1993.

CEB Bulletin Number 187 (1988), *Concrete Structures under impact and Impulsive Loading - Synthesis Report.*

Wittmann, F.H. K. Rokugo, E. Bruhwiler, H. Mihashi, and P. Simonin, (1988) “Fracture Energy and Strain Softening of Concrete as Determined by Means of Compact Tension Specimens,” *Materials and Structures*, Volume 21, pages 21-32.